
KADIR HAS UNIVERSITY
SCHOOL OF GRADUATE STUDIES
DEPARTMENT OF ELECTRONICS ENGINEERING

# MULTI-SENSOR INDOOR POSITIONING

TARIK AYABAKAN

DOCTOR of PHILOSOPHY THESIS

İSTANBUL, JANUARY, 2022

# MULTI-SENSOR INDOOR POSITIONING

TARIK AYABAKAN

A thesis submitted to
the School of Graduate Studies of Kadir Has University
in partial fulfilment of the requirements for the degree of
Doctor of Philosophy in
Electronics Engineering

Istanbul, January, 2022

# APPROVAL

This thesis titled MULTI-SENSOR INDOOR POSITIONING submitted by TARIK AYABAKAN, in partial fulfillment of the requirements for the degree of Doctor of Philosophy in Electronics Engineering is approved by

Prof. Dr. Feza Kerestecioğlu (Advisor) .....
Kadir Has University

Assoc. Prof. Dr. Taner Arsan .....
Kadir Has University

Assoc. Prof. Dr. Osman Kaan Erol .....
Istanbul Technical University

Prof. Dr. Serhat Erküçük .....
Kadir Has University

Asst. Prof. Dr. Ahmet Cezayirli .....
Fenerbahçe University

I confirm that the signatures above belong to the aforementioned faculty members.

.....
Prof. Dr. Mehmet Timur Aydemir
Dean of School of Graduate Studies
Date of Approval: 11/01/2022

## DECLARATION ON RESEARCH ETHICS AND PUBLISHING METHODS

I, TARIK AYABAKAN; hereby declare

- that this Ph.D. Thesis that I have submitted is entirely my own work and I have cited and referenced all material and results that are not my own in accordance with the rules;
- that this Ph.D. Thesis does not contain any material from any research submitted or accepted to obtain a degree or diploma at another educational institution;
- and that I commit and undertake to follow the "Kadir Has University Academic Codes and Conduct" prepared in accordance with the "Higher Education Council Codes of Conduct".

In addition, I acknowledge that any claim of irregularity that may arise in relation to this work will result in a disciplinary action in accordance with university legislation.

TARIK AYABAKAN

.....

11/01/2022

*To my dear wife and lovely daughter*

*Özgül & Bade*

# ACKNOWLEDGEMENT

I would like to thank my advisor Prof. Dr. Feza KERESTECİOĞLU for his support and endless patience during my academic studies. He always enlightened my way to accomplish my thesis.

I also would like to thank Assoc. Prof. Dr. Taner Arsan and Assoc. Prof. Dr. Osman Kaan Erol for their peerless support. I also want to thank Kadir Has University administration for providing me full scholarship. It was a great honor for me to serve as a teaching assistant during my doctorate studies at Kadir Has University.

Finally, I wish to express my appreciation to my family. It would not be possible to produce this thesis without their great support.

# ABSTRACT

In this study, multi-sensor indoor positioning methods, which fuse the tri-laterated position data of the target are considered. The lateration is based on the distances that are obtained using the signal strengths received from different Wi-Fi access points. A new method, which is based on federated Kalman filtering (FKF) and makes use of the fingerprint data, namely, federated Kalman filter with skipped covariance updating (FKF-SCU) is proposed for indoor positioning. After that challenging issue of FKF, information sharing coefficient assignment is studied and two online adaptation methods based on received signal strength indication (RSSI) and distance information gathered from APs are proposed. Lastly, FKF-SCU structure is combined with adaptive FKF configuration. The data collected on two different test beds are used to compare the performance of the proposed positioning methods to those of the regular federated and centralized filters. It is shown on the test data that these algorithms improve the position accuracy and provide fault tolerance whenever signal reception is interrupted from an access point.

**Keywords: Indoor positioning, federated Kalman filter, sensor fusion, fault tolerance**

# ÖZET

Bu çalışmada, hedefin üçgenlenmiş konum bilgilerini birleştiren, çoklu sensörlü kapalı alanda konumlandırma metodlarına yer verilmiştir. Üçgenleme işlemi Wi-Fi erişim noktalarından alınan sinyal gücünün çevrimi ile elde edilen mesafe bilgileri ile gerçekleştirilmiştir. Yeni bir yöntem olarak, Federe Kalman Filtresine (FKF) dayanan ve parmak izi verilerini kullanan, Federe Kalman Filtresi-Kovaryans Güncellemesi Atlama (FKF-KGA) yöntemi sunulmuştur. Sonrasında FKF yapısında zorlu konulardan biri olan, bilgi paylaşım katsayısı atama problemi için iki yeni uyarlanabilir yöntem sunulmuştur. Bu yöntemler erişim noktalarından elde edilen, alınan sinyal gücü göstergesi ve mesafe bilgilerine dayanarak geliştirilmiştir. Son olarak, FKF-KGA yapısı uyarlanabilir bilgi paylaşım katsayı yöntemleri ile birleştirilmiştir. İki farklı kapalın alanda toplanan gerçek veriler, sunulan federe filtre yapıları ile standart federe ve merkezileştirilmiş süzgeç yapılarının performanslarını karşılaştırmak için kullanılmıştır. Test verileri ile gerçeklenen benzetimler sonunda, sunulan yöntemlerin konum doğruluğu ve erişim noktasında sinyal kaybı durumundaki hata toleransında iyileşme sağladığı gözlenmiştir.

**Anahtar sözcükler: Kapalı alanda konumlandırma, federe Kalman filtresi, sensör füzyonu, hataya toleranslık**

# TABLE OF CONTENTS

# LIST OF FIGURES

# LIST OF TABLES

# LIST OF SYMBOLS

| | |
|---|---|
| $\mathbf{d}_i$ | distance of the target from $i$th access point |
| $\mathbf{e}(k)$ | measurement residual |
| $\mathbf{H}(k)$ | system matrix of measurement model |
| $\mathbf{H}_i(k)$ | system matrix of measurement model for $i$th local filter |
| $\mathbf{K}(k)$ | Kalman gain |
| $\mathrm{n}_p$ | path loss exponent |
| $\mathbf{P}(k\|k-1)$ | error covariance matrix of the predicted estimate |
| $\mathbf{P}(k\|k)$ | error covariance matrix of the filtered estimate |
| $\mathbf{P}_i(k\|k-1)$ | error covariance matrix of the predicted estimate of $i$th local filter |
| $\mathbf{P}_i(k\|k)$ | error covariance matrix of the filtered estimate of $i$th local filter |
| $\mathbf{P}_g(k\|k)$ | global error covariance matrix of the federated Kalman filter |
| $P_r$ | received signal power (dBm) |
| $P_0$ | reference signal power(dBm) |
| $p_x(k)$ | $x$-coordinate of the position of the target at instant $k$ |
| $p_y(k)$ | $y$-coordinate of the position of the target at instant $k$ |
| $\mathbf{Q}$ | system noise covariance matrix |
| $\mathbf{Q}_i$ | system noise covariance matrix of $i$th local filter |
| $\mathbf{Q}_g$ | global system noise covariance matrix of the federated Kalman filter |
| $\mathbf{R}$ | measurement noise covariance matrix |
| $\mathbf{R}_i$ | measurement noise covariance matrix of $i$th local filter |
| $R_r$ | received signal power |
| $R_t$ | transmitted signal power |
| $R_0$ | reference signal power |
| $\mathbf{x}$ | two dimensional position vector |
| $\mathbf{x}(k)$ | system state vector |
| $\mathbf{x}_i$ | location of access points |
| $\mathbf{x}_i(k)$ | state vector of ith local system |
| $\hat{\mathbf{x}}(k\|k-1)$ | predicted estimate of the state vector |

| | |
|---|---|
| $\hat{\mathbf{x}}(k\|k)$ | filtered estimate of the state vector |
| $\hat{\mathbf{x}}_\mathbf{i}(k\|k)$ | filtered estimate of the state vector of $i$th local filter |
| $\hat{\mathbf{x}}_\mathbf{i}(k\|k-1)$ | predicted estimate of the state vector $i$th local filter |
| $\hat{\mathbf{x}}_\mathbf{g}(k\|k)$ | global estimate of the federated Kalman filter |
| $X_\sigma$ | zero-mean Gaussian random variable |
| $\mathbf{v}(k)$ | zero mean white measurement noise |
| $\mathbf{v}_i(k)$ | zero mean white noise of $i$th measurement |
| $v_x(k)$ | $x$-coordinate of the velocity of the target at instant $k$ |
| $v_y(k)$ | $y$-coordinate of the velocity of the target at instant $k$ |
| $\mathbf{w}(k)$ | zero mean white system noise |
| $\mathbf{w}_i(k)$ | zero mean white noise of $i$th system |
| $\mathbf{w}_{p,x}(k)$ | zero mean white system noise |
| $\mathbf{z}(k)$ | measurement vector |
| $\mathbf{z}_i(k)$ | measurement vector ith local system |
| $\beta_i$ | information sharing coefficient ith local filter |
| $\beta_h$ | information sharing coefficient assigned with highest value |
| $\beta_l$ | information sharing coefficient assigned with lowest value |
| $\beta_m$ | information sharing coefficient assigned according to $\beta_l$ and $\beta_m$ |
| $\sigma$ | standard deviation |
| $\mathbf{\Phi}(k)$ | system matrix of system model |

# LIST OF ACRONYMS AND ABBREVIATIONS

| | |
|---|---|
| AOA | Angle of Arrival |
| AP | Access Point |
| BLE | Bluetooth Low Energy |
| CDF | Cumulative Distribution Function |
| CKF | Centralized Kalman Filter |
| DKF | Decentralized Kalman Filter |
| DR | Dead Reckoning |
| FKF | Federated Kalman Filter |
| FKF-SCU | Federated Kalman Filter with Skipped Covariance Updating |
| GLONASS | Global Navigational Satellite Systems |
| GNSS | Global Navigation Satellite Systems |
| GPS | Global Positioning System |
| INS | Inertial Navigation System |
| IPS | Indoor Positioning System |
| KF | Kalman Filter |
| LF | Local Filter |
| LOS | Line of Sight |
| NLOS | Non-Line of Sight |
| PDR | Pedestrian Dead Reckoning |
| RFID | Radio Frequency Identification |
| RSSI | Received Signal Strength Indication |
| RTOF | Round Trip of Flight |
| SKF | Single Kalman Filter |
| TB | Test Bed |
| TDOA | Time Difference of Arrival |
| TOA | Time of Arrival |

# 1. INTRODUCTION

## 1.1 Navigation and Positioning

The purpose of navigation is to direct the movement of a vehicle to a given destination. Navigation problems can be classified according to the location of the target under two contexts, namely, as outdoor and indoor. If the target is moving outdoors, its positioning or navigation is done easily via different kinds of Global Navigational Satellite Systems (GNSS). There are four different GNSS in use all over the world, which are Global Positioning System (GPS) operated by the USA, Global Navigation Satellite System (GLONASS) operated by Russia, European GNSS Galileo, and China's GNSS BeiDou. Among these GNSS technologies, GPS is the widely used system and thanks to advances in GPS, such applications for outdoor purposes became abundant. For the localization of the target holding a GPS embedded device, mainly two information are needed. The first one is the distance between GPS devices and GPS satellites. The second one is the position of GPS satellites. When these two pieces of information is available, the target location can be obtained using lateration methods [1].

However, in some situations, GPS signals may not be available for localization. A car traveling through a tunnel is a good example for this case. Once there is no use of GPS due to the inadequacy or complete loss of satellite signals, alternative systems are needed to get accurate position information [2]. Generally, an Inertial Navigation System (INS) is the choice to keep the system to provide position information in the absence of a GPS signal. Integration of INS and GPS also provides improvement in overall system accuracy and reliability that could not be attained just using only one of them. Hence, when a set of states (position, velocity, etc.) can be estimated via more than one sensor, not only accuracy increases but also reliability of the system improves [3].

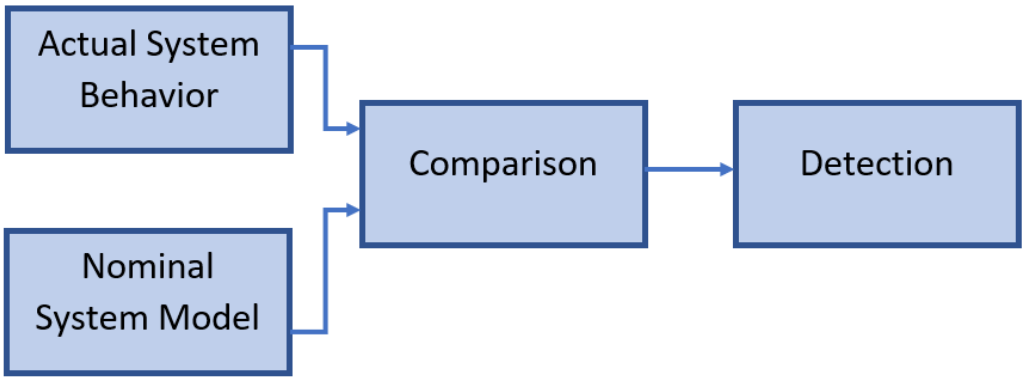


**Figure 1.1** Fault detection via system comparison

## 1.2 Fault Tolerance

In every system, the occurrence of a fault is an inevitable situation. Therefore, a vital part of system design criteria is system reaction in case of a fault. Fault tolerance means the ability of a system to go on operating within acceptable limits despite the occurrence of a fault. Fault tolerance is achieved as a combination of fault detection and isolation mechanisms, and remedies overcoming these faults. It is useful to understand if everything is fine or something has gone wrong with the operation of a system. Detecting the existence of fault correctly at an appropriate time is called fault detection and diagnosis. This step is the most important step for fault-tolerant system. Because undetected faults may cause severe problems. In literature, fault detection and diagnosis is also named as *fault detection and isolation* or *fault detection and identification*. But in this study, we will use fault detection and identification. A fault detection system compares system attitude with nominal behavior and if a deviation occurs from what is expected, it is detected and the detection system alerts. After detection of the fault, there are generally three identification methods; model-based, knowledge-based and model-free (empirical or signal processing) methods [4, 5]. In this study, the model-based method shown in Figure 1.1 will be used to compare the output of the actual system with the nominal system data. Fingerprint data will be our nominal system data. [6].

On the other hand, we can classify faults according to their occurrence with respect to time. While designing a fault-tolerant system we need to consider the occurrence of faults related to time given in Figure 1.2. Because, it may occur intermittently, abruptly or incipiently [6]. Among these models, we used the abrupt signal loss as a faulty scenario. In this scenario, signal loss occurs at one of the Access Points (APs) and one could not get information from the failed AP for a while.

After detection and identification of the fault, re-configuration of the faulty system may achieve the overall system to be fault-tolerant by preventing the error propagation to other subsystems. This can be provided by combining the information obtained from different sensors that estimate common states (position, velocity etc.) of the system. By that way, not only system ambiguity is decreased, but also robustness and fault tolerance is increased [7]. Such a fault tolerance can be obtained, for example, using an INS/GPS combination. If in some situations (e.g., car traveling through a tunnel) GPS signals get lost, a navigation application can continue to provide positioning information by using the inertial sensor of the mobile device in the absence of GPS signals [2]. In this study, a similar fault scenario is applied to assess the fault tolerance performance of the proposed multi-sensor indoor positioning method.

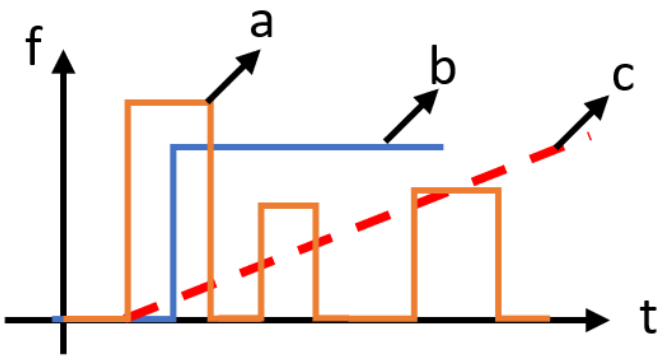


**Figure 1.2** Time-dependency of faults: (a) intermittent, (b) abrupt, (c) incipient

## 1.3 Indoor Positioning

For both, military and nonmilitary applications, GPS is the essential source to get position information. But, since the construction of buildings with concrete walls act as an obstacle for GPS signals so that these signals lose strength in penetrating beyond the walls. Therefore, due to the low signal quality of GPS signals indoors, they are not usable for indoor applications. Hence, an alternative sensor that can be used for indoor area application is needed; and many studies focused on designing systems that are as reliable as GPS is for outdoor applications [8, 9, 10, 11, 12, 13]. There are many alternative sensors to be used as information sources for indoor environment applications such as Wi-Fi, BLE, beacons, RFID, UWB etc., and different methods to process these information to facilitate positioning such as Time of Arrival (TOA), Time Difference of Arrival (TDOA), Received Signal Strength Indication (RSSI) etc [14]. Among these methods RSSI is used widely for localization. In a line of sight situation, it may provide good results while calculating the distance between the signal source and target. But in real world, there are many factors affecting the propagation of RSSI signals at indoor environments. Therefore, RSSI measurements are not reliable to use for localization directly [15, 16]. Hence, extra tools are needed to facilitate positioning by using RSSI.

Given the reliability problem of RSSI signals, fault tolerant indoor positioning system is aimed to provide a reliable accuracy performance by using RSSI measurements of APs. Even though Kalman Filtering and its variants are widely used for combining different sensor measurements at outdoor localization and navigation applications, none of the existing methods or sensors appear as to be favored against others for the indoor case [17, 18, 19]. A method that can be applied as widely as GNSS for outdoor environment is still an open area for research. Considering its effective and dominant usage in outdoor applications, Kalman filtering and its derivatives can be seen as a promising means towards this aim.

## 1.4 Data Fusion

The process of measurement data integration is called as *data fusion* [20] and can find applications in many areas [3, 21, 22]. Regardless of the source, where the data comes from, Kalman Filtering which is originally proposed in [23] is one of the most commonly used tools in outdoor positioning systems and can also be applied for data fusion. Different variants of Kalman Filter, such as extended, unscented, decentralized and federated filters can find applications for positioning purposes.

In early applications, Kalman Filter is used for astronautical guidance systems and became a part of the Apollo project on board guidance. In mid 1960's Kalman filter solved for an aviation company the *data fusion* problem of radar and inertial sensor information to obtain aircraft trajectory estimate. After that time, it has become an indispensable part of the modern navigation systems [2] .

Different sensor information can be fused mainly with, centralized filtering or decentralized filtering structures [24]. In centralized structure, sensor measurements are combined at one step and in one filter for the required output. Whereas, in decentralized structure the sensor measurements are fused in two steps. At the first step, sensor measurements are filtered by different sensor-dedicated *sub*-filters. Then, solutions gathered from these sub-filters are combined in another filtering component, which produces the *global* result. In [25, 26], these filtering configurations are compared for indoor environment. Results of this study presents that more accurate positioning can be obtained with a multi-sensor configuration as compared to single-sensor one. Moreover, promising results are obtained from decentralized structure.

A centralized structure that is applied for data fusion is the Centralized Kalman Filter (CKF). CKF is simple to apply with its one-step data processing and highly accurate output can be obtained with very small information loss. Nevertheless, the computational load increases for high-dimensional state vectors.

Moreover, if a fault occurs at one of the sensors, the performance degradation rise by the time and badly effects the general system performance [27, 28].

Therefore, in view of this disadvantage of CKF, a two-stage data-processing decentralized filtering structure can be proposed. In a Decentralized Kalman Filter (DKF), parallel working sensor-dedicated independent local filters (LFs) provide locally optimal solutions and these results are combined in a master filter to get the globally optimal solution. Main advantage of this structure is that the failure of one of the sensors, whose data are processed in a parallel way, does not cause a total failure at the overall system output, but only some performance degradation may occur [29, 30, 31, 24]. However, despite the great attention DKF has received, it also could not provide a fault-tolerant performance as desired [31]. This fact motivated the introduction of federated filtering configurations to surmount theoretical restrictions and constraints in applications of CKF and DKF. In [32] and [33], an *information-sharing* methodology complying with conversation of information is applied to DKF. This structure is called Federated Kalman Filter (FKF).

In the literature, there are some indoor positioning studies aiming to fuse information gathered from the sensors by using a centralized filtering structure [34, 35, 36, 37] and very few studies considering FKF structure [38, 39]. But, none of them take into account fault tolerance issues.

### 1.5 Literature review

Indoor positioning systems has drawn great attention in recent years. Different kinds of methods are used to localize the target position. These methods have pros and cons by themselves; but the main purpose is to find accurate position of the user. Microsoft organized Indoor Localization Competition in 2014 and [17] published the results, experiences and lessons gathered. At that competition, 22 different solutions are put in test. As a result, there is no technology or a combination of technologies that gives satisfied performance as GPS provides for outdoors, yet.

Therefore, we can say that Indoor Localisation Problem is still not solved and needs more investigation. Another important result of that competition is that there is not a single solution working perfectly in all indoor environments. Hence, the best solution for indoor positioning might be a hybrid one, which can adapt itself to different kinds of situations. In that study, 22 different indoor localization studies were evaluated. As a result, it is shown that Wi-Fi based approaches can achieve accuracy below 1m.

In [14], a comprehensive overview of the systems and techniques used for indoor localization was provided. The authors focused their analyses on widely-used triangulation, scene analysis, and proximity methods. They also discussed a commonly-used IPS method, fingerprinting, in detail. They simulated many methods and compared performances according to accuracy, precision, complexity, scalability, robustness and cost. As future work, it is emphasized that hybrid algorithms are needed. Furthermore, wireless sensors used together with other technologies such as optical (e.g., IR), inertial, dc electromagnetic and ultrasonic for indoor location is another trend.

In [40] IPS on a special topic as IPS for Pedestrians were reviewed. There are many technological advances making systems applicable. Sensors and processing nodes used in IPS design became smaller and these improvements in size of sensors helped the designer to focus on Pedestrian Dead Reckoning (PDR) systems. In this study, techniques for step detection, characterisation, inertial navigation and step-and-heading-based dead-reckoning are reviewed and compared.

The Personal Network (PN) concept is provided in [8]. PNs are designed to form one network in distinct locations. PNs' design is based on the requirements of the users and PNs evaluate the users' technological devices by providing connections between each other. This paper provides an extensive survey of many IPSs, which include both commercial products and research solutions. These systems are assessed in

scope of cost, accuracy performance, robustness, complexity, commercial availability, and limitations.

In [41] many papers were reviewed and a survey of the mathematical methods used for position estimation in IPS is provided. Their study focused especially on methods used with radio frequency signals. They analysed the techniques in four groups: Geometry-based methods, minimization of cost functions, fingerprinting, and Bayesian techniques. They also evaluated each technique according to the applicability, requirements, and immunity to non-line-of-sight (NLOS) propagation of the signals.

Another IPS method, "Optical Positioning", is studied in [42]. Receive and transmit sensors of the optical communication get many improvements both for accuracy and size. Their dimensions became smaller and their data transmission rates increased by technological advances. After that many people started studying optical sensor for indoor positioning. Mautz and Tilch summarized 26 different approaches and provided the key parameters of the optical systems. As a summary, high accuracy performance of optical indoor positioning approaches is emphasized which is between a couple of $\mu$m and dm. At the end of the study to improve performance of the optical positioning system data fusion with other sensors is suggested.

In [43] rising interest in the indoor positioning system design were emphasized. This study is especially on indoor wireless tracking of mobile nodes, which estimates a series of correlated locations of mobile nodes. Also, there are many studies and applications using Visible Light Communication as information source. Philips company has already completed 17 case studies that were put into use in Italy, France, Belgium, Netherlands, Dubai, South Africa etc. Philips published white paper about their study and take attention usage of LEDs in indoor positioning and indoor location services.

In [44], an Indoor Visible Light Communication Positioning System by using a different technique named RF Carrier Allocation is introduced. They have reached a

few centimeters of positioning accuracy. Details of their study and simulation results can be seen in [44].

A survey on Visible Light Positioning studies can be found in [45]. They compared 17 different studies according to their technology, backbone network, cost, driver and accuracy. Among the discussed techniques, Spatial Division Multiple Access is the most capable technology thanks to its low complexity and usage of smartphones own cameras. On the other hand, there are some challenging issues about VLP such as the refresh rate of camera, the processing time of the images effecting the position update and avoidance of flicker occurrence. Until now we have talked about many different techniques using different information sources. By using just one system to get position information of the target may not provide good accuracy in every environment. Therefore, to get better accuracy data fusion must be used. There are many studies to enhance the performance by combining the data of two or more IPS systems.

In [19], an improved BLE (Bluetooth Low Energy) indoor localization with data fusion based on Kalman Filtering was designed. In this study, BLE beacon set is used as an information source and different mobile devices are used to design a highly accurate indoor positioning system. Performance of the designed system is compared with other indoor positioning technologies. Main objective of this study was chosen as examining how accurate the proposed method is, as well as interaction of the obstacles to localization and direction of the mobile system antenna. To obtain a more accurate positioning information, a hybrid method, which fuses dead reckoning and trilateration methods via Kalman filter, was studied. By that fusion, the pros and cons of the individual methods were shown. In their study, they declared that constraints of trilateration and dead reckoning methods can be overcome with proposed hybrid method. Simulation results showed a positioning error performance of less than one meter. Moreover, the proposed method is found to be fault tolerant in case of a failure at the localization mechanism.

In [46] an indoor positioning method based on Probabilistic RFID Map and Kalman Filtering was proposed. Multilateration is used to estimate location of unknown RFID tag. The proposed algorithm is independent from the readers position information which provides practical usage. After many simulations, they achieved accurate localization. But the only disadvantage of that algorithm is requiring many RSS measure samples to achieve good accuracy.

In [47] the aim was to design a fault tolerant positioning system to enhance reliability instead of accuracy in fault-free conditions. They introduced different fault models and investigated fault tolerance performance of positioning methods they have used. They evaluated the performance as the percentage of corrupted signal strength measurements increases. By these models, they tried to catch the effect of fails or attacks and described how to simulate them using real test data at the end they analyzed the distance solutions in KNN method, discussed alternative solutions and studied the performance in the occurrence of faults.

A Fault Tolerant IPS based on fingerprint method was proposed by [48]. They used Subtract on Negative Add on Positive (SNAP) algorithm in their study and tried to enhance accuracy and fault tolerance performance. SNAP algorithm is simply based on the idea that if an AP is detected, then the user is more likely to reside in the locations inside the Region of Convergence (ROC) that have similar RSS values to the observed RSS value. There is a modified version of SNAP algorithm named SNAPz algorithm also focuses on neighboring or remaning zones of detected AP's. If an AP is detected with certain RSS value, the target may be located with higher probability in the zone where the reference locations have RSS values or with some probability with neigboring zone or with low probability in the remaining zones. They used different kind of fault models mostly causing from APs during their work. As a result, they got an improvement in both positioning accuracy and fault tolerance.

In [49], fault tolerant indoor localization using Wi-Fi was studied. It is assumed that there is not a relationship between the occurrence of faults/failures at Access Points. This assumption is a limitation on the faults. For example, power failures affect all the APs at the same time but this situation is not considered. In order to detect faults Wi-Fi enabled devices are deployed at various positions to monitor status of APs.

As can be seen from the studies presented, there are many methods used to design IPS. Earlier studies were mostly about getting position information with high accuracy. But more recently, it was realized that accurate position information does not make sense by itself. Because indoor experimental areas are different almost for each study. Then, an indoor localization system cannot be generalized for public use like GPS for outdoor. Hence IPS design by using two or more sensor became a vital issue to make systems more reliable, adaptive and fault tolerant. Still, more effort is needed in designing fault tolerant IPS, which is the focus of this thesis.

## 1.6 Outline and Original Contributions

In this study, different sensor fusion methods based on Kalman Filter are proposed for indoor positioning. Following the introduction, localization methods used for indoor environments are given in Chapter 2. Signals follow a path while radiating in an environment. Parameters of the signal propagation model differs at each environment and these parameter values directly effect the positioning performance. In literature, they are treated as experimentally obtained values; but they are used as constant values regarding the general structure of the environment such as obstruction in the building, line-of-sight area etc. Considering the different nature of each environment for accurate localization, in Section 2.7 of this study, signal propagation model parameters are estimated with a least squares approach for each AP. Even if the signal propagation is modelled and the parameters are estimated, distance information converted from received signal power, namely, RSSI cannot be used as is for positioning applications. Hence, extra tools are needed to process RSSI data.

On the other hand, better accuracy can be achieved by a fusion of data gathered from different sensors. In this thesis, Kalman filter is used for these operations. General information about the Kalman filter and its steps are given in Chapter 3.

Data fusion methods used for indoor positioning is stated at Chapter 4. Fault tolerance is one of the design criteria for outdoor positioning systems. But it is still not a widely studied issue in indoor positioning. With this motivation, a fault tolerant indoor positioning method, namely, Federated Kalman Filter with Skipped Covariance Updating (FKF-SCU) algorithm is proposed and details of this algorithm is given in Section 4.4.

Moreover in Section 4.5, another contribution is given as proposing two adaptation methods for FKF information sharing coefficients. In FKF, assigning information sharing coefficients with their appropriate values is a challenging topic. To solve this problem for indoor environment, proposed adaptation methods are used for the simulations with collected data in indoor area without any faulty scenario. Better positioning results are obtained with proposed adaptation methods as compared to equal information sharing.

Finally, in Section 4.6, information coefficient adaptation methods are used with FKF-SCU by considering the faulty scenario. It is seen that these two proposed methods can work cooperatively. On the other hand, fault tolerant indoor positioning system with adaptive information structure provided slightly better results than a structure with equal information sharing.

Initially, performances of traditional CKF and FKF are compared to asses multi-sensor structure for indoor area by using generated data. Proposed methods given at Chapter 2 are assessed with different sets both with generated synthetic data and data, which were originally collected at two different real indoor environment. Simulation results given in Section 5.1 showed that multi-sensor structures provide better performance than the system using only one sensor measurement.

After simulations with synthetic data, in Section 5.3 fault detection and fault tolerance issues are considered as one of the main contribution of this study. During simulations a faulty scenario is generated for collected real data at two different indoor environments. Fault tolerance performance of FKF and CFK is assessed and Federated Kalman Filter with Skipped Covariance Updating, namely, FKF-SCU algorithm is proposed. Moreover good results are obtained with proposed FKF-SCU algorithm.

After all simulations, it is deduced that proposed methods provide improvements in the sense of fault tolerance and positioning accuracy. Moreover these methods can be used with already deployed access points and do not require server to process data. Finally, Chapter 6 concludes this thesis and proposes some future areas for research.

# 2. INDOOR POSITIONING METHODS

## 2.1 Introduction

Indoor positioning received great attention in recent years. Its application areas also widened in parallel to that increase of popularity. Huge buildings, hospitals, shopping malls, airports, warehouses are some of the places that are used for indoor localization applications. There are different methods that can be used to localize or track a target in an indoor environment. In this section, definitions of the proximity, triangulation, fingerprint and dead-reckoning methods, which are commonly employed for indoor localization and are classified in Figure 2.1. These methods evaluate data gathered from sensors such as bluetooth beacons, Wi-Fi access points, Radio Frequency Identification (RFID) tags or badges, etc., to get information of the target via RF, ultrasound, infra-red signal or visible light [13, 50, 51, 52, 53]. In the sequel, all such sensor will be referred as access points (AP).

## 2.2 Proximity

Proximity is regarded as the simplest method to obtain information about the target location [43]. Namely, the position of the target is determined as the known position of the AP, which is detecting the target. It is possible that the target is detected by more than one access points. In that case, its position is matched to the AP having the strongest signal. This technique does not require any time synchronization among access points; but provides low position accuracy [54]. In [55], this method is used with RFID tags for an IoT study, while a proximity detection system is proposed in [56] by using acoustic signals.

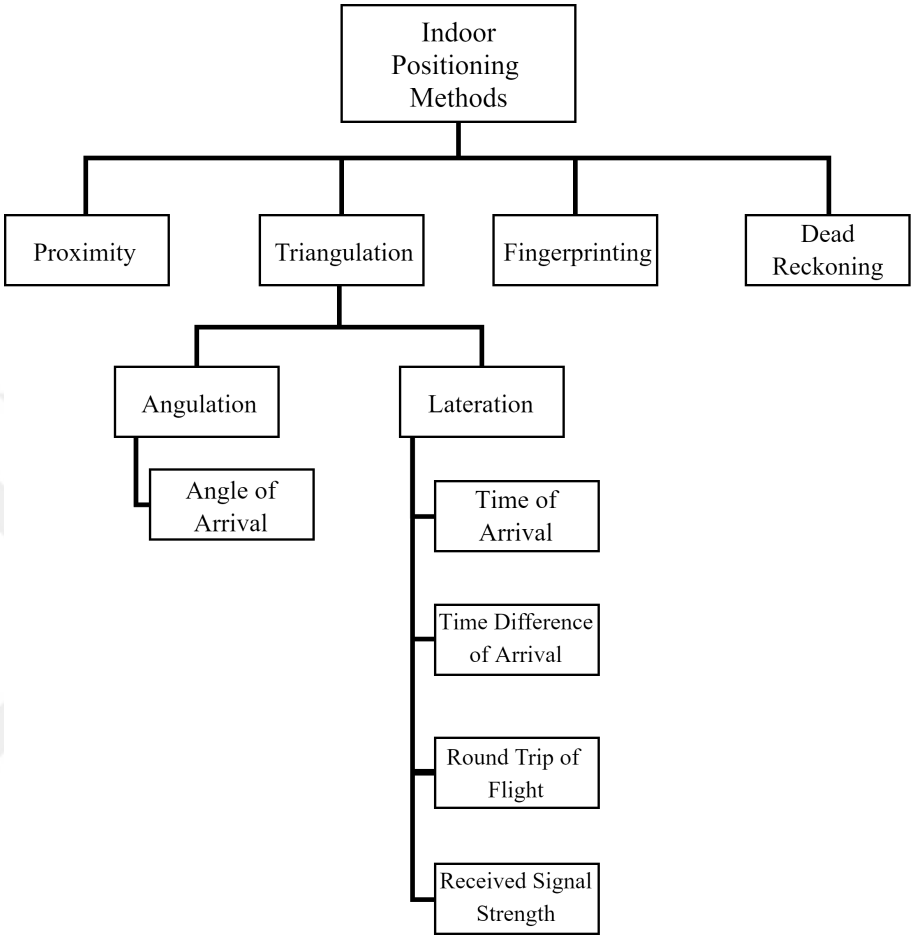


**Figure 2.1** Indoor positioning methods

## 2.3 Triangulation

The triangulation is a localization method, in which the geometric properties of triangles are used to localize the target. In order to get position data of the target we can either use angle or distance measurements from the sensors. Finding a position by using the relative angles of sensors as seen from the target is called angulation. On the other hand, the method based on the distances between access points and target is called lateration [57].

### 2.3.1 Angulation

The Angle-of-Arrival (AOA) measurements are also known as the direction of arrival or bearing measurements in literature [14]. In the AOA technique, angle of received signal is estimated from at least two sources. Then, from the intersection of the angle line for each signal source location is found. In two dimensional case, two AOA's are sufficient to find the location. But, directivity of the antenna, multipath propagation and shadowing may severely effect accuracy of the position estimate. Hence, LOS is needed for accurate measurement [1, 54].

### 2.3.2 Lateration

Lateration method uses distance information between the target (i.e., the mobile device) and sensors to locate the target as shown in Figure 2.2. The distance information can be obtained by different techniques, such as Time of Arrival (TOA), Time Difference of Arrival (TDOA), Round Trip of Flight (RTOF) and Received Signal Strength (RSS).

### 2.3.3 Time of arrival

This method estimates the distance by measuring the travel time of the signal between transmitter and receiver. The speed of light is then used to convert the time-difference information to the distance information. The distance to at least three signal sources can then be used to find the location of the target as the intersection point of the circles centered at the signal sources and having radii equal to these distances, respectively. Time synchronization between the transmitters and the receiver is required for the accuracy of this method [1, 20].

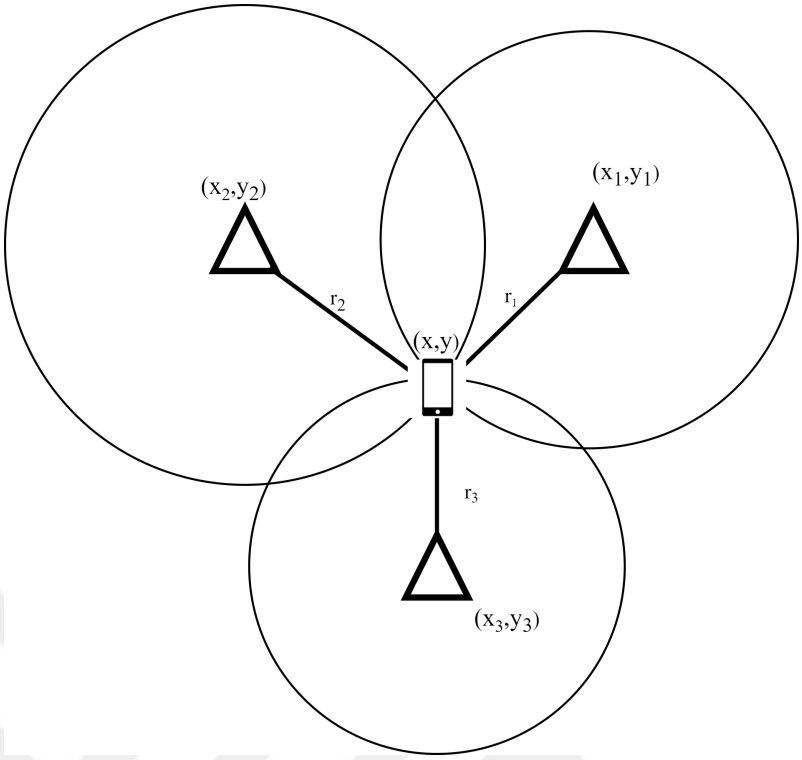


**Figure 2.2** Lateration method

### 2.3.4 Time difference of arrival

Time Difference of Arrival (TDOA) enhances the accuracy of TOA. If an accurate time synchronization is not provided between transmitters and receivers, distance information will not be accurate in TOA [1]. TDOA does not need synchronization between transmitter and receiver. However, synchronization between transmitters is needed. Position is calculated with the time difference of arrival of a signal sent by at least three transmitters and received by the target [54].

### 2.3.5 Round-trip time of flight

Round-Trip Time of Flight method use the travel time of a signal from source to target and turning back. Distance calculation is the similar to TOA, but does not require synchronization between the devices as in TOA [58].

### 2.3.6 Received signal strength

Received Signal Strength indication (RSSI) is a measure of the RF energy received and is closely related to the distance between the transmitter and the receiver. In RSS-based algorithms, the target that is to be tracked measures the strength of signals received from the transmitters. Then, these signal strengths are used to estimate the distance between the transmitters and receivers. By this way, the receiver can estimate its position with respect to the transmitter nodes. This method does not require time synchronization between target and transmitters.Therefore, RSS-based algorithms are widely used in indoor positioning [59, 60, 61, 62, 63]. A propagation model relating RSS to the distance is presented in Section 2.6.

## 2.4 Fingerprinting

As mentioned above, multipath phenomenon drastically effects the accuracy of RSS-based algorithms. Location of a target can also be obtained via fingerprinting technique, which consists of an offline training phase, and an online localization phase. The database of reference positions is built in the training phase by storing the received signal strength from deployed access points. The location of the target is estimated by matching the location data to the training data [13, 64]. Practical difficulty of this method is that creating a fingerprint database requires huge effort and cost related to measurements, calibration, site planning, etc. Furthermore, the collected fingerprints need to be updated whenever a new item is added or removed in area. As a result, this technique may not be suitable for every indoor environment [1].

## 2.5 Dead Reckoning

Dead reckoning (DR) systems use sensors on the target to estimate its position with respect to known initial position. For example, in [19], an accelerometer is used for step detection and a magnetometer is used for heading estimation of the target to

calculate dead reckoning location in a hybrid system. Because of their cumulatively increasing error characteristics, DR techniques are used in conjunction with other methods to obtain hybrid systems.

From the definitions of techniques given above, we can infer that to get location information of the target, there are mainly two steps. First, signal measurements must be made to determine quantities such as signal strength, angle information or time data, etc. Then, target location is calculated by using these quantities gathered at first step. If proximity method is applied, measurements can be made at or outside the target. It is also possible to measure angle of arrival both at target and sensor. TOA, TDOA and RTOF are all time-based methods; however, they differ on where the localization can be performed. Measurement can be made both at target or access points if TOA technique is used. On the other hand, positioning calculation is only possible at the target, for TDOA. Lastly, it is also possible to make these calculations at target with RTOF-capable Wi-Fi access points. In this study proximity, triangulation and fingerprinting methods are used at different steps of proposed configurations. Main positioning calculations are performed with distance based lateration method of triangulation. To do this, RSS is used to get distance information. On the other hand, one of the FKF information sharing coefficient adaptation is based on proximity method and fingerprint method is used to estimate parameters of signal propagation model and to define fault detection rule.

## 2.6 Indoor Positioning Using RSSI

In this study, lateration-method kind of triangulation is used among indoor positioning methods shown in Figure 2.1. Lateration method is based on the distance between target and AP. Distance information is calculated with RSS measurements. RSS measurements can be easily gathered from already deployed information sources via open source software without requiring extra hardware and easily converted to distance. Another important reason choosing that method is that there is no need time synchronization between sensors and target.

In this section, conversion of RSS measurements to distance information will be described. Following collection of RSSI data, the range between the access points and the target can be determined by using these RSSI measurements. Then, these distance information are used for a lateration to localize the target. If three information sources are used, this process is called *tri-lateration*; in case of more than three sources, it is called *multi-lateration*.

The two-dimensional position vector of the target can be denoted as $\mathbf{x} = [x \quad y]^T$ and location of the deployed access points can be denoted as $\mathbf{x}_i = [x_i \quad y_i]^T$ $(i = 1, 2, \ldots, N)$. Then the squared-distances of the target from the access points can be calculated with the equations given as [1],

$$\begin{aligned} d_1^2 &= (\mathbf{x} - \mathbf{x}_1)^T(\mathbf{x} - \mathbf{x}_1) \\ d_2^2 &= (\mathbf{x} - \mathbf{x}_2)^T(\mathbf{x} - \mathbf{x}_2) \\ &\vdots \\ d_N^2 &= (\mathbf{x} - \mathbf{x}_N)^T(\mathbf{x} - \mathbf{x}_N). \end{aligned} \tag{2.1}$$

If there are more than two APs in an indoor environment, for $N > 2$, the position of the target can be calculated from this set of equations by subtracting the first equation from the others.

$$\begin{aligned} d_1^2 - d_2^2 &= -2\mathbf{x}_1^T\mathbf{x} + \mathbf{x}_1^T\mathbf{x}_1 + 2\mathbf{x}_2^T\mathbf{x} - \mathbf{x}_2^T\mathbf{x}_2 \\ d_1^2 - d_3^2 &= -2\mathbf{x}_1^T\mathbf{x} + \mathbf{x}_1^T\mathbf{x}_1 + 2\mathbf{x}_3^T\mathbf{x} - \mathbf{x}_3^T\mathbf{x}_3 \\ &\vdots \\ d_1^2 - d_N^2 &= -2\mathbf{x}_1^T\mathbf{x} + \mathbf{x}_1^T\mathbf{x}_1 + 2\mathbf{x}_N^T\mathbf{x} - \mathbf{x}_N^T\mathbf{x}_N. \end{aligned} \tag{2.2}$$

Then, by rearranging equations in (2.2),

$$\begin{bmatrix} 2\mathbf{x}_2^T - 2\mathbf{x}_1^T \\ 2\mathbf{x}_3^T - 2\mathbf{x}_1^T \\ \vdots \\ 2\mathbf{x}_N^T - 2\mathbf{x}_1^T \end{bmatrix} \mathbf{x} = \begin{bmatrix} d_1^2 - d_2^2 + \mathbf{x}_2^T\mathbf{x}_2 - \mathbf{x}_1^T\mathbf{x}_1 \\ d_1^2 - d_3^2 + \mathbf{x}_3^T\mathbf{x}_3 - \mathbf{x}_1^T\mathbf{x}_1 \\ \vdots \\ d_1^2 - d_N^2 + \mathbf{x}_N^T\mathbf{x}_N - \mathbf{x}_1^T\mathbf{x}_1 \end{bmatrix}. \tag{2.3}$$

the resulting $N-1$ equations can be written as [18]

$$\mathbf{C}\mathbf{x} = \mathbf{D}, \tag{2.4}$$

where

$$\mathbf{C} = 2\begin{bmatrix} (\mathbf{x}_2 - \mathbf{x}_1)^T \\ (\mathbf{x}_3 - \mathbf{x}_1)^T \\ \vdots \\ (\mathbf{x}_N - \mathbf{x}_1)^T \end{bmatrix} \quad \text{and} \quad \mathbf{D} = \begin{bmatrix} d_1^2 - d_2^2 + \mathbf{x}_2^T\mathbf{x}_2 - \mathbf{x}_1^T\mathbf{x}_1 \\ d_1^2 - d_3^2 + \mathbf{x}_3^T\mathbf{x}_3 - \mathbf{x}_1^T\mathbf{x}_1 \\ \vdots \\ d_1^2 - d_N^2 + \mathbf{x}_N^T\mathbf{x}_N - \mathbf{x}_1^T\mathbf{x}_1 \end{bmatrix}. \tag{2.5}$$

Therefore, the target position is obtained as

$$\mathbf{x} = (\mathbf{C}^T\mathbf{C})^{-1}\mathbf{C}^T\mathbf{D}. \tag{2.6}$$

One can get the position of the target via Equation (2.6) on condition that $\mathbf{C}$ is of full column rank. For $N > 3$, the position vector $\mathbf{x}$ can be obtained by multi-lateration. Also, the localization can be done via tri-lateration by employing different methods such as taking the mean of tri-lateration measurements or considering best three RSSI measurements [19].

On the other hand, the distance between the target and APs can be computed with reference to the received signal strength. By denoting the received and transmitted signal powers as $R_r$ and $R_t$, respectively, one can relate received signal power to distance $d$ to the transmitting AP as

$$R_r(d) = R_t \cdot \left(\frac{1}{d}\right)^{n_p}, \tag{2.7}$$

where $n_p$ is the path loss exponent that reflects the rate, at which the RSS decreases with distance, as well as representing the multi-path effect [18]. Further, let us denote the reference signal power at a reference distance $d_0$ from the transmitter by $R_0$. In other words,

$$R_0 = R_t \cdot \left(\frac{1}{d_0}\right)^{n_p} \tag{2.8}$$

Hence, one can express, the received signal power for line-of-sight environment as

$$R_r(d) = R_0 \cdot \left(\frac{d_0}{d}\right)^{n_p} \tag{2.9}$$

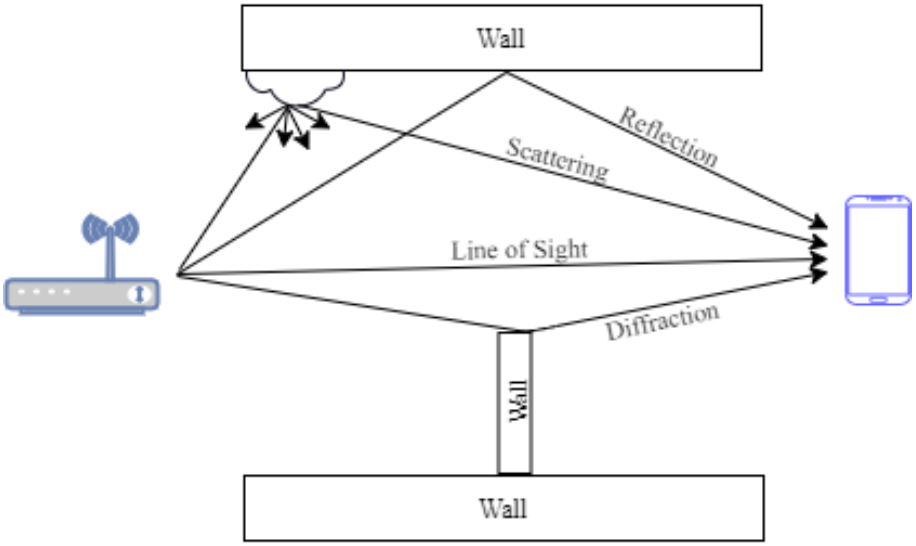


**Figure 2.3** Error sources in indoor signal reception

or

$$10 \log R_r(d) = 10 \log R_0 - 10 n_p \log \left( \frac{d}{d_0} \right). \tag{2.10}$$

However, propagation of received signal is not always line of sight. Because of the structure of indoor environment, walls,objects etc. signal propagation is effected. Then signal may reflect, scatter of diffract as shown in Figure 2.3. Hence in order to get reliable distance data, these disturbances must be considered and appropriate signal propagation model must be defined.

Defining $P_r = 10 \log R_r$ and $P_0 = 10 \log R_0$ as received and reference signal powers measured in dBm, and representing the effect of fading by $X_\sigma$, a zero-mean Gaussian random variable with standard deviation $\sigma$, a log-normal shadow model [65, 66, 67] for the received power can be written as

$$P_r = P_0 - 10 n_p \log \left( \frac{d}{d_0} \right) + X_\sigma, \tag{2.11}$$

which is a commonly used propagation model for indoor environments. Note that for the line-of sight test beds or environments $X_\sigma$ is accepted as zero.

For a unity reference distance, (2.11) further simplifies to

$$P_r = P_0 - 10 n_p \log(d) + X_\sigma \tag{2.12}$$

and the distance between the target and an AP can be computed as

$$d = 10^{(P_0 - P_r + X_\sigma)/(10n_p)} \tag{2.13}$$

once the parameters $P_0$, $n_p$ and $X_\sigma$ are determined. The path loss parameter is 2, i.e., the power is inversely proportional to the square of the distance, for free space. Nevertheless, it may vary substantially according to the environment as shown in Table 2.1. One can also estimate the path loss component via (2.12) for a specific environment by collecting the reference power, received power and distance data using

$$n_p = \frac{P_0 - P_r + X_\sigma}{10\log(d)}. \tag{2.14}$$

The parameter $X_\sigma$ is accepted as zero for targets, which are in the line of sight. However, for non-line-of-sight cases, this parameter is generally determined by experimentally. As a result more precise values of $X_\sigma$ and $n_p$ parameters need to be gathered for better positioning accuracies.

## 2.7 Estimation of Model Parameters

Lateration is one of the widely used distance-based positioning method and we need to know estimated or exact distance between the signal source AP and target to be localized. In indoor environments, RSSI measurements gathered from APs can be converted to distance information by using (2.13). Here $P_0$ and $P_r$ are reference and received signal powers obtained from signal source but $n_p$ and $X_\sigma$ are unknown parameters. Moreover, these parameters are not constant for every environment and can vary significantly regarding to the target location. In [19, 68], $X_\sigma$ and $n_p$ are defined as values pertaining to entire area, which have to be obtained experimentally. In this study, least squares method is used to estimate these parameters. Moreover, they are calculated separately for each AP, instead of considering an average value for $n_p$, which is assumed to be valid for whole localization environment.

To obtain a least-square estimates $n_p$ and $X_\sigma$, let us rewrite (2.12) as

$$P_0 - P_r = 10n_p\log(d) - X_\sigma \tag{2.15}$$

**Table 2.1** Path Loss Exponents for Different Environments

| Environment | Path Loss Exponent |
|---|---|
| Free Space | 2 |
| Urban Area Cellular Radio | 2.7-3.5 |
| Line-of-Sight in Building | 1.6-1.8 |
| Obstruction in Building | 4-6 |

or

$$y = \boldsymbol{\varphi}^T \boldsymbol{\theta} \tag{2.16}$$

with

$$y = P_0 - P_r, \qquad \boldsymbol{\varphi} = \begin{bmatrix} 10\log(d) \\ -1 \end{bmatrix}, \qquad \boldsymbol{\theta} = \begin{bmatrix} n_p \\ X_\sigma \end{bmatrix} \tag{2.17}$$

If $P_0$ and measurement data for $P_r$ ($P_{ri}$, $i = 1, \ldots, n$) are available for different distances $d_i$, collecting them in a matrix form, one can estimate $n_p$ and $X_\sigma$ as

$$\begin{bmatrix} n_p \\ X_\sigma \end{bmatrix} = (\boldsymbol{\Delta}^T \boldsymbol{\Delta})^{-1} \boldsymbol{\Delta}^T \begin{bmatrix} P_0 - P_{r1} \\ P_0 - P_{r2} \\ \vdots \\ P_0 - P_{rn} \end{bmatrix}, \tag{2.18}$$

where

$$\boldsymbol{\Delta} = \begin{bmatrix} 10\log(d_1) & -1 \\ 10\log(d_2) & -1 \\ \vdots & \vdots \\ 10\log(d_n) & -1 \end{bmatrix}. \tag{2.19}$$

Once these parameters are estimated, the distance between the target and APs can be calculated using (2.13).

## 2.8 Conclusion

In this chapter, main algorithms used for indoor positioning are described. Pros and cons of these algorithms are also given. After that, the algorithm, which will

be used for localization of the target is detailed. If there is connection with wireless APs deployed in indoor environment, it is easy to read RSS information of these APs namely RSSI with open source mobile phone applications or software. These RSSI readings are very useful to get distance information between target and APs and infere which AP is closest and which one is farthest to the target. From that RSSI measurements distance between Wi-Fi and target can be calculated via (2.13). However, indoor environment is really complex for radio signal propagation if there is not a line-of-sight situation. Because of the disturbing effects of people, walls, objects located in indoor environment, signal reliability decreases. Therefore, an appropriate propagation model must be defined by considering the disturbances. Moreover, parameters in the (2.13), that is extracted from the propagation model in (2.11), plays vital role for the accuracy quality of the distance information. These parameters differ for each environment as given at Table 2.1 and can be calculated via (2.14) that is $X_\sigma = 0$ for line of sight situation. However, most of the time the indoor environment is at non-line of sight situation. In scope of these reasons, a least square method based model parameter estimation method is proposed. However, this is not enough to use RSSI measurements solely to get position information. Therefore, we need additional filtering to improve accuracy of position information.

# 3. KALMAN FILTER AND ITS VARIATIONS

## 3.1 Introduction

There are many methods used for both outdoor and indoor navigation. These methods do not have same performance and they have their advantages and disadvantages. Outdoor navigation has two important sensors GPS and INS. We have GPS sensor in our smartphones, which we can enable and track our position anytime if situations are good enough to communicate with GPS satellites. Our smartphones also have MEMS, accelerometer and gyroscope. Kalman Filter is the main method used to obtain location information from these sensors. Most of the navigation systems (nearly all of them) use Kalman Filter. Traditional Kalman Filter has different variants such as extended, unscented, decentralized and federated etc. For outdoor navigation Kalman Filter is the most dominant method but for indoor positioning there is not a mostly used method and sensor yet. Hence, one of the main aims of the studies about indoor positioning is to design a widely used system like GPS for outdoor navigation. Still, there is not a unique system or method that we can apply for every indoor place. Studies lasting more than ten years about indoor positioning show that to achieve more accurate and more reliable solution we need to fuse information gathered from sensors to get position information [14, 19, 34, 35, 36, 38]. The aim of data fusion is to get more accurate information than that is already gathered from any individual data source, using a combination of data obtained from various sources. By that way, uncertainty in measured data can be also decreased by utilizing the complementary properties of different data sources.

## 3.2 Kalman Filter Equations

The Kalman filter is a highly effective and adjustable tool for combining noisy sensor outputs to get a state estimation of system, which may have ambiguity in its dynamics. Rudolph Kalman introduced his famous filter in 1960 and practically implemented it for the first time for integrating an inertial navigator with airborne radar. Nowadays, there are many methods used for navigation; but nearly all of them are variants of Kalman filter [2].

In order to apply Kalman Filter first we need to have system and measurement models as given below

$$\mathbf{x}(k+1) = \mathbf{\Phi}(k)\,\mathbf{x}(k) + \mathbf{w}(k) \tag{3.1}$$

$$\mathbf{z}(k) = \mathbf{H}(k)\,\mathbf{x}(k) + \mathbf{v}(k) \tag{3.2}$$

Here $\mathbf{\Phi}(k)$ denotes system matrix and $\mathbf{x}(k)$ is the state vector. $\mathbf{H}(k)$ denotes system matrix and $\mathbf{z}(k)$ is the measurement vector, whereas $\mathbf{w}(k)$ defines a zero mean white system noise with covariance matrix $\mathbf{Q}$ and $\mathbf{v}(k)$ is white measurement noise with zero mean and covariance matrix $\mathbf{R}$. The system and measurement noises, $\mathbf{v}(k)$ and $\mathbf{w}(k)$, are assumed to be uncorrelated and

$$\mathbf{Q} = \mathbf{E}[\mathbf{w}(k)\mathbf{w}^T(k)], \mathbf{w}(k) \sim N(0, \mathbf{Q}) \tag{3.3}$$

$$\mathbf{R} = \mathbf{E}[\mathbf{v}(k)\mathbf{v}^T(k)], \mathbf{v}(k) \sim N(0, \mathbf{R}) \tag{3.4}$$

$$\mathbf{E}[\mathbf{w}(k)\mathbf{v}^T(k)] = 0 \tag{3.5}$$

After defining system and measurement models, Kalman Filter process is conducted in two steps, prediction and update, which can be expressed as follows [28]:

Prediction (Time Update):

$$\hat{\mathbf{x}}(k|k-1) = \mathbf{\Phi}(k-1)\hat{\mathbf{x}}(k-1|k-1) \tag{3.6}$$

$$\mathbf{P}(k|k-1) = \mathbf{\Phi}(k-1)\mathbf{P}(k-1|k-1)\mathbf{\Phi}(k-1)^T + \mathbf{Q}(k-1) \tag{3.7}$$

Update (Measurement Update):

$$\mathbf{K}(k) = \mathbf{P}(k|k-1)\mathbf{H}^T(k)[\mathbf{H}(k)\mathbf{P}(k|k-1)\mathbf{H}^T(k) + \mathbf{R}(k)]^{-1} \quad (3.8)$$

$$\hat{\mathbf{x}}(k|k) = \hat{\mathbf{x}}(k|k-1) + \mathbf{K}(k)[\mathbf{z}(k) - \mathbf{H}(k)\hat{\mathbf{x}}(k|k-1)] \quad (3.9)$$

$$\mathbf{P}(k|k) = [\mathbf{P}^{-1}(k|k-1) + \mathbf{H}(k)\mathbf{R}^{-1}(k)\mathbf{H}^T(k)]^{-1} \quad (3.10)$$

In first step of the Kalman Filtering structure $\hat{\mathbf{x}}(k|k-1)$ defines best estimate based on information till step $k-1$ and in second step filtered estimate of $\mathbf{x}(k)$ is provided with $\hat{\mathbf{x}}(k|k)$ by taking into account measurements.

In (3.9), the predicted state estimate $\hat{\mathbf{x}}(k|k-1)$ gathered via (3.6) and the measured data obtained from the system is used to compute the filtered estimate $\hat{\mathbf{x}}(k|k)$ so as to minimize the mean-square estimation error. Then, this filtered estimate is used to compute the predicted estimate $\hat{\mathbf{x}}(k|k-1)$ of the next step as in (3.6). The matrix $\mathbf{K}(k)$ is the so-called Kalman gain and $\mathbf{P}(k|k-1)$ and $\mathbf{P}(k|k)$ are the error covariance matrices of the predicted and filtered estimates, which are defined as

$$\mathbf{P}(k|k-1) = E\left\{[\mathbf{x}(k) - \hat{\mathbf{x}}(k|k-1)][\mathbf{x}(k) - \hat{\mathbf{x}}(k|k-1)]^T\right\} \quad (3.11)$$

and

$$\mathbf{P}(k|k) = E\left\{[\mathbf{x}(k) - \hat{\mathbf{x}}(k|k)][\mathbf{x}(k) - \hat{\mathbf{x}}(k|k)]^T\right\}, \quad (3.12)$$

respectively.

The Kalman filter is a two-step process as shown in (3.6)-(3.10) . The "prediction" step is also called as "Time Update" step in other studies. This step updates the estimate and estimation uncertainty, considering the effects of uncertain system dynamics over the times between measurements. The "Measurement Update" step is also called "correction step". This step updates the estimate itself and the covariance matrix of estimation uncertainty, based on measurement information. Here Kalman gain weights measurement residual or namely innovation $\mathbf{e}(k)$ given in (3.13) and weighted measurement residual is combined with predicted state estimate for calculation of new state estimate.

$$\mathbf{e}(k) = \mathbf{z}(k) - \mathbf{H}(k)\hat{\mathbf{x}}(k|k-1) \quad (3.13)$$

Innovation $\mathbf{e}(k)$ has measurement prediction covariance as given below

$$\mathbf{S}(k) = E\left\{[\mathbf{z}(k) - \mathbf{H}(k)\hat{\mathbf{x}}(k|k-1)][\mathbf{z}(k) - \mathbf{H}(k)\hat{\mathbf{x}}(k|k-1)]^T\right\} \quad (3.14)$$

and

$$\mathbf{S}(k) = \mathbf{H}(k)\mathbf{P}(k|k-1)\mathbf{H}^T(k) + \mathbf{R}(k), \quad (3.15)$$

By considering (3.8) and (3.15) together Kalman gain can be written again as

$$\mathbf{K}(k) = \mathbf{P}(k|k-1)\mathbf{H}^T(k)[\mathbf{S}(k)]^{-1} \quad (3.16)$$

From this relationship one can deduce that Kalman gain $\mathbf{K}(k)$ is large in case of inaccurate prediction and small in case of inaccurate measurement.

### 3.3 Alternative Kalman Filter Configurations

When measurements for estimated states of the system are gathered from different sensors, there are also different filtering configurations to combine these measurements to get system output. Sensors can be configured mainly with centralized and decentralized structure. If the sensor measurements are combined via one Kalman filter with one dynamic model at one step, it is called centralized Kalman filter (CKF). On the other hand, it is also possible to combine multi-sensor information at two stages. In first stage data processing is conducted at each local sensor dedicated Kalman filters. After that local solutions are combined by a master filter. This structure is called decentralized Kalman filter (DKF) [30]. CKF and DKF are both provide good accuracies but none of them have superiority on fault tolerance. DKF is proposed especially to eliminate faul tolerance disadvantage of CKF. But couldn't achieve expected performance. Then in [32] a new decentralized Kalman filter structure with information sharing approach is proposed as federated Kalman filter (FKF). The term information generally denotes to global state vector and inverse of covariance matrix,namely information matrix, obtained at main filter output. Main difference of FKF is its information sharing property and different FKF configurations are also provided according to the information sharing strategy,

which are zero-reset feedback, partial fusion feedback, full fusion feedback and no-reset feedback. In full fusion feedback mode, global estimate and covariance matrix solution obtained at overall system output is fedback to local filters. Therefore performance improvement can be seen at less accurate local filter solution as a result of this global solution reset. With this resetting, full fusion feedback provides most accurate estimates among other configuration. In no-reset feedback mode, overall system solution is not fedback to local filters and each local filters work independently having accuracies closer to their general level. Among these four configurations no-reset feedback structure is proposed as having lowest accuracy but most fault-tolerant configuration [32, 69]. Another important issue in federated Kalman filter is how to share information among local filters. Information is shared according to the sharing coefficients and that coefficients must sum to unity in accordance with conversation of information. But there is not a definite rule to assign values for sharing. As a result, appropriate coefficients must be defined so as to enhance performance of configurations mentioned above.

## 3.4 Conclusion

In this chapter, a widely used estimation algorithm for navigation and positioning applications, namely, Kalman Filter is detailed with its equations. Ever since its been introduced, it became a basic tool to solve navigation and positioning problems. However, the usage of Kalman Filter is not restricted to its original representation. By the time different variants are proposed regarding to the requirements of the systems. It can provide estimate with single sensor measurement but main application area is fusing information gathered from different sensors. Then in next section, different Kalman Filtering structures used for indoor positioning will be given.

# 4. DATA FUSION FOR INDOOR POSITIONING

## 4.1 Introduction

Kalman Filter is used in many positioning and navigation applications for outdoor environments. Nevertheless, that popularity is not same for indoor environment. On the other hand, for outdoor navigation, Kalman Filter is the most dominant method. But, for indoor positioning, none of the existing methods and sensors appear as to be favoured against others. Hence, one of the main aim of the studies about the indoor positioning is to design a widely used system like GPS for outdoor navigation. After reviewing many studies, we have seen that there is not a unique system or method that we can apply for every indoor place. Instead, we can use a method that combines the systems already occurring in indoor locations.

In this section, we describe proposed methods, which are applied for localization of the target and algorithms that implement this method on the gathered information. Target localization is based on the RSSI information coming from APs; a technique widely used for indoor environments [59, 60, 61, 62, 63]. An important issue here is the reliability of the RSSI signals. This issue is studied in [15] and it is deduced that RSSI can easily be disturbed and, therefore, cannot be used as they are, for calculating target location in an indoor environment. So, we need extra measures to enhance positioning accuracy.

## 4.2 Centralized Kalman Filter

Once we have at least two systems that can provide data, the information gathered from these systems can be easily fused by combining them in a single vector form and using Kalman Filter algorithm. When there are measurements from $N$ sensors,

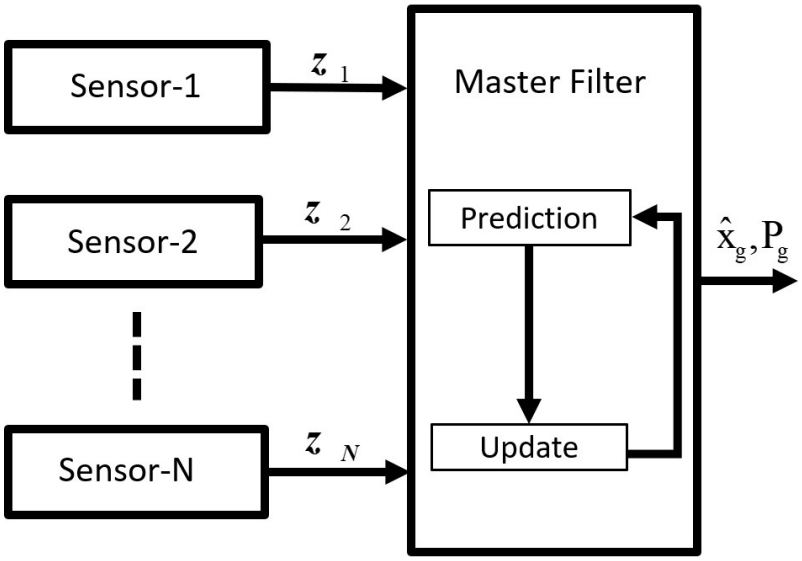


**Figure 4.1** Centralized Kalman filter structure

(3.2) can be rewritten as

$$\mathbf{z}_i(k) \;=\; \mathbf{H}_i(k)\,\mathbf{x}(k) + \mathbf{v}_i(k),\; i = 1, 2, \ldots, N. \tag{4.1}$$

Here, $\mathbf{z}_i$ denotes measurement information from different sensors and $\mathbf{H}_i$ is the measurement matrix. A filter combining these measurements in single vector measurement structure and performing Kalman Filter steps in (3.6)–(3.10) is known as *centralized filter*. General representation of CKF is as shown in Figure 4.1. Its implementation is simple and it yields low data loss. However, its computational load increases as the dimension of the state vector becomes higher. Moreover, a fault that arise in one of the sensors will degrade the overall system output. Although abruptly occurring high-level faults may be easily detected, faults, which increase gradually in time may go undetected. The detection of such faults may be delayed and, until the detection, data coming from the faulty sensor will still be accepted for the computation of the system output [28].

### 4.3 Federated Kalman Filter

CKF has a simple structure with high accuracy but it has drawbacks especially at fault tolerance. Then, around 1980's a two-stage data processing decentralized filtering structure received great attention. But, many studies showed that DKF

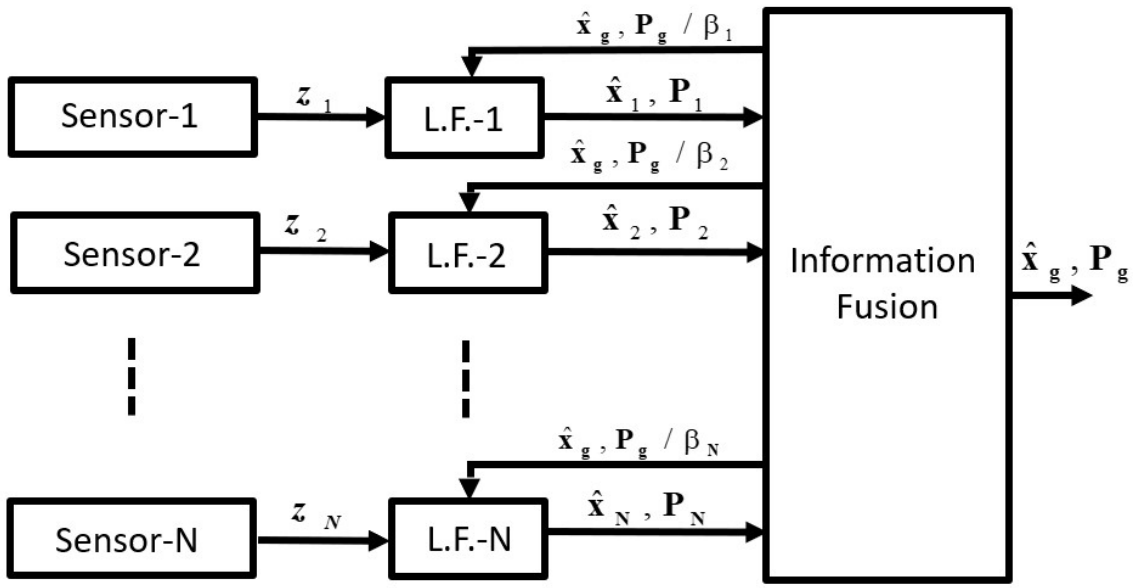


**Figure 4.2** Federated Kalman filter resetting structure

structure decreased the computational load of CKF but could not provide desired fault tolerance performance.

After that, in order to overcome such drawbacks of CKF and DKF, Carlson proposed the Federated Kalman Filtering method in [32, 33]. Contrary to CKF, in FKF measurement information are not combined in a single vector. In FKF, related to its federated structure, each sensor has dedicated local Kalman Filters at which the state estimation is performed by processing data from each sensor separately. After completion of local estimations, these estimates are fused to get a global estimate, as shown in Figure 4.2. The "information-sharing" methodology was applied to DKF and provided the effective Federated Kalman Filter (FKF) basically in three steps.

İn FKF, initially the total system information is shared among the LFs regarding to information sharing coefficients. These information are generally process noise, initial condition and/or common measurement information [31]. After information sharing, Kalman filter time-update and measurement-update steps in (3.6)–(3.10) are performed for each LF. Finally, these updated LF output information are combined in a master filter to obtain a global estimate and its covariance matrix.

During FKF process, the output estimation $\hat{\mathbf{x}}_g$ is shared with LFs and the system noise matrix $\mathbf{Q}_g$ and estimation covariance matrix $\mathbf{P}_g$ is divided between LFs. That information division is applied according to the sharing coefficients, which should satify the conservation of information principle by adding up to unity [31, 32, 33]. Information sharing principle for $N$ local sensors can be expressed as

$$\sum_{i=1}^{N} \beta_i = 1. \tag{4.2}$$

In a federated filter, firstly, information sharing is done as

$$\begin{aligned}
\mathbf{P}_i^{-1}(k-1|k-1) &= \beta_i \, \mathbf{P}_g^{-1}(k-1|k-1) && (4.3)\\
\mathbf{Q}_i^{-1} &= \beta_i \, \mathbf{Q}_g^{-1} && (4.4)\\
\hat{\mathbf{x}}_i(k-1|k-1) &= \hat{\mathbf{x}}_g(k-1|k-1) && (4.5)
\end{aligned}$$

for $i = 1, 2, \ldots, N$. After resetting the local systems by these information, Kalman Filtering equations are applied for them. Therefore, predictions and updates of LFs are done as

$$\begin{aligned}
\hat{\mathbf{x}}_i(k|k-1) &= \mathbf{\Phi}(k-1)\hat{\mathbf{x}}_i(k-1|k-1) && (4.6)\\
\mathbf{P}_i(k|k-1) &= \mathbf{\Phi}(k-1)\mathbf{P}_i(k-1|k-1)\mathbf{\Phi}^T(k-1) + \mathbf{Q}_i(k-1) && (4.7)\\
\mathbf{K}_i(k) &= \mathbf{P}_i(k|k-1)\mathbf{H}_i^T(k) \\
&\quad \times[\mathbf{H}_i(k)\mathbf{P}_i(k|k-1)\mathbf{H}_i^T(k) + \mathbf{R}_i(k)]^{-1} && (4.8)\\
\hat{\mathbf{x}}_i(k|k) &= \hat{\mathbf{x}}_i(k|k-1) + \mathbf{K}_i(k)[\mathbf{z}_i(k) - \mathbf{H}_i(k)\hat{\mathbf{x}}_i(k|k-1)] && (4.9)\\
\mathbf{P}_i(k|k) &= [\mathbf{P}_i^{-1}(k|k-1) + \mathbf{H}_i^T(k)\mathbf{R}_i^{-1}(k)\mathbf{H}_i(k)]^{-1}. && (4.10)
\end{aligned}$$

for $i = 1, 2, \ldots, N$. Finally, local updates are combined to get the global solution using

$$\begin{aligned}
\mathbf{P}_g^{-1}(k|k) &= \sum_{i=1}^{N} \mathbf{P}_i^{-1}(k|k) && (4.11)\\
\hat{\mathbf{x}}_g(k|k) &= \mathbf{P}_g(k|k)[\sum_{i=1}^{N} \mathbf{P}_i^{-1}(k|k)\hat{\mathbf{x}}_i(k|k)]. && (4.12)
\end{aligned}$$

Relationship between local and global filters can be seen at equations (4.11) and (4.12). Here, first local optimal estimates are obtained from the outputs of local

filters. Secondly, these local optimal results are combined at the master filter and best global result is obtained. Then, global results are shared among LFs to continue with the next filtering step [32].

### 4.4 Federated Kalman Filter with Skipped Covariance Updating

As mentioned above, FKF combines fault tolerant advantage of decentralized structure with information sharing principle. Moreover, the global estimate computed via (4.11) and (4.12) resets the estimates of LFs with (4.5).

Estimation accuracy performance of the LFs can be improved with this resetting operation even if individual estimations may still have less accuracy as compared to the global estimate [69]. Resetting may seem very useful in normal operation of the system. But, this resetting operation may badly effect the system performance in case of a faulty situation. If a fault occurs at one of the sensors, not only the global estimate is affected by the LF processing the faulty sensor; but also the estimate performance of all other LFs degrade because of the resetting operation. Moreover, the degradation will persistently spread to the future estimates even if the faulty sensor returns to its normal operation mode. In order to overcome a long term performance degradation in the global estimate because of a faulty sensor, we propose to skip the covariance matrix update of the LFs in (4.10) and fuse the information coming from the LFs by

$$\mathbf{P}_g^{-1}(k|k) = \sum_{i=1}^{N} \mathbf{P}_i^{-1}(k|k-1) \tag{4.13}$$

$$\hat{\mathbf{x}}_g(k|k) = \mathbf{P}_g(k|k)[\sum_{i=1}^{N} \mathbf{P}_i^{-1}(k|k-1)\hat{\mathbf{x}}_i(k|k)]. \tag{4.14}$$

instead of (4.11) and (4.12). In other words, the fusion step is applied using the predicted covariance matrices and not the filtered ones. Since we choose a small $\beta$, which is close to zero for resetting, small amount of the system noise and estimation error covariance $\mathbf{Q}_g$ and $\mathbf{P}_g$ are shared to the related local filter in view of (4.3) and (4.4). After that, predicted covariance is calculated with these matrices, which attains a large value, and hence, its inverse being small. On the other hand, because

of the small magnitude of $\mathbf{P}_i^{-1}(k|k-1)$, filtered covariance matrice is dominated by $\mathbf{H}_i^T(k)\mathbf{R}_i^{-1}(k)\mathbf{H}_i(k)$. Moreover, we cannot give less weight to the faulty local estimates at (4.12) as desired to suppress its effect to global estimate. Hence, we skip the computation of the filtered covariance and fuse local estimates using the predicted covariances. Obviously, whenever a fault is detected, $\beta_i$'s in (4.3) and (4.4) can be adapted so as to weight the faulty AP minimally, too.

Additionally, once offline RSSI measurements namely fingerprints of the target environment are already collected, faults occurring at sensors can be detected by using statistical properties, such as mean ($\mu$) and standard deviation ($\sigma$) of these fingerprint values. On the other hand, if fingerprints of the environment are not available, an experimentally determined constant threshold can be used for fault detection purposes.

The complete algorithm that uses a federated Kalman filter with skipped covariance updating (FKF-SCU) is depicted in Figure 4.3.

## 4.5 Adaptation of Information Sharing Coefficients

It is possible to enhance LFs accuracy performance by feeding back the global result with resetting structure of the FKF. But, a fault at any of the local sensors may lead to adverse effects in the overall performance of the system. Different filtering structures such as no-reset, fusion-reset, zero-reset and filter-rescale modes, which vary in their schemes of information sharing are proposed in [69]. In no-reset mode estimate, outputs of local filters are not reset with the global estimate output of the master filter. The no-reset configuration of federated filter is advantageous in scope of fault tolerance among other configurations. Hence, we also used no-reset configuration of the federated filter to asses performance of this structure.

Information sharing coefficients are the main difference of FKF from, both, CKF and the decentralized filter. Information sharing coefficients directly effect local filter accuracy and fault tolerance performance of the overall system. Since there is not

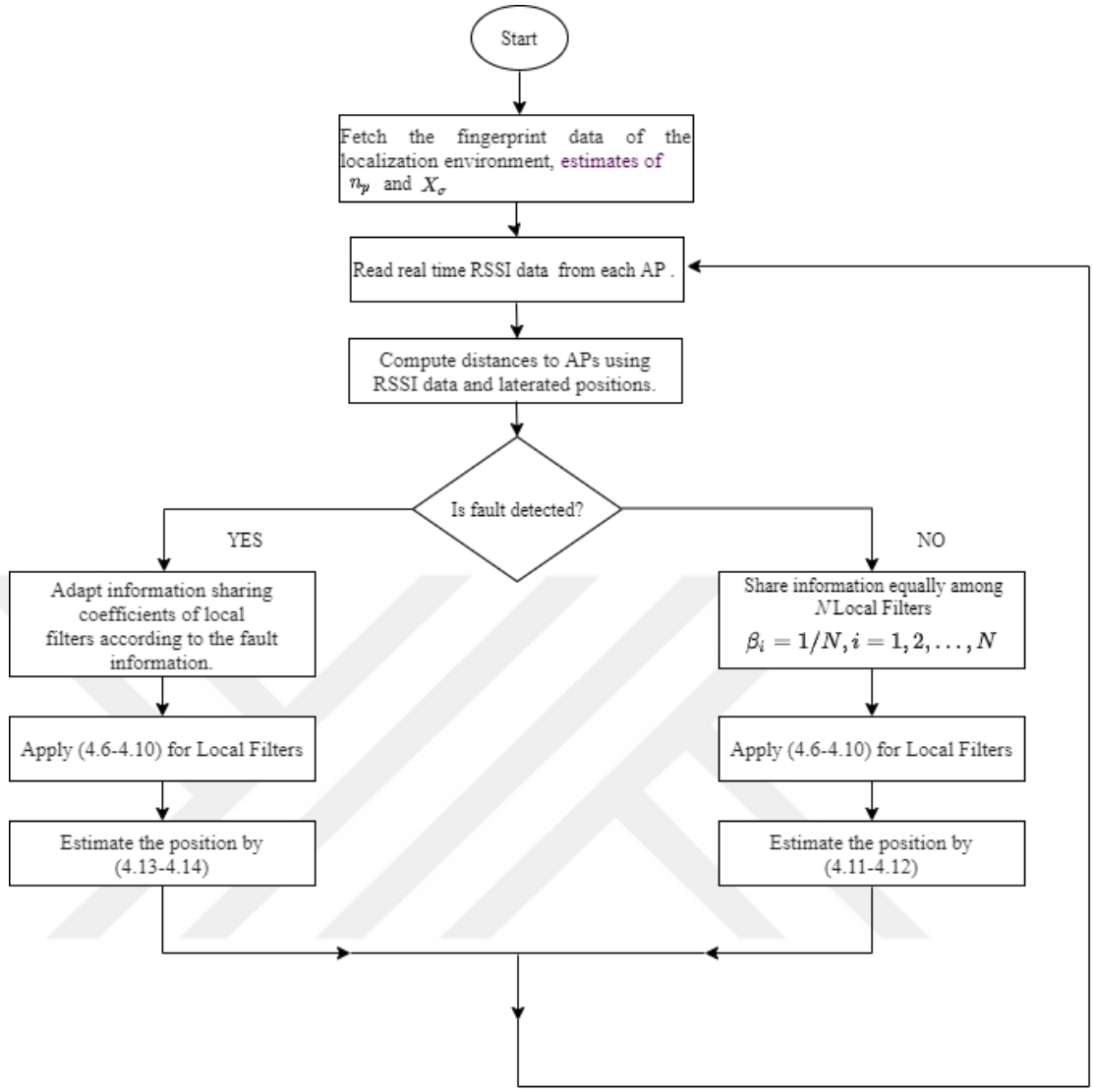


**Figure 4.3** Fault tolerant positioning algorithm using FKF-SCU

a definite rule in literature to assign information sharing coefficients, at this point we need to stress that the challenge in FKF design is the selection of a suitable set of information sharing coefficients. The only thing known about these coefficients is that if $\beta_i = 1/N$ $(i = 1, \ldots, N)$, i.e. local estimates are fused equally weighted, FKF performs as good as CKF [32]. For indoor environments, any a priori knowledge about the target positioning area may be used to determine the values of the $\beta_i$'s in order to improve the positioning performance. Moreover, online adaptation of these coefficients may be also possible using the RSSI data and can be combined with a no-reset structure as shown in Figure 4.4. Below, we propose two approaches

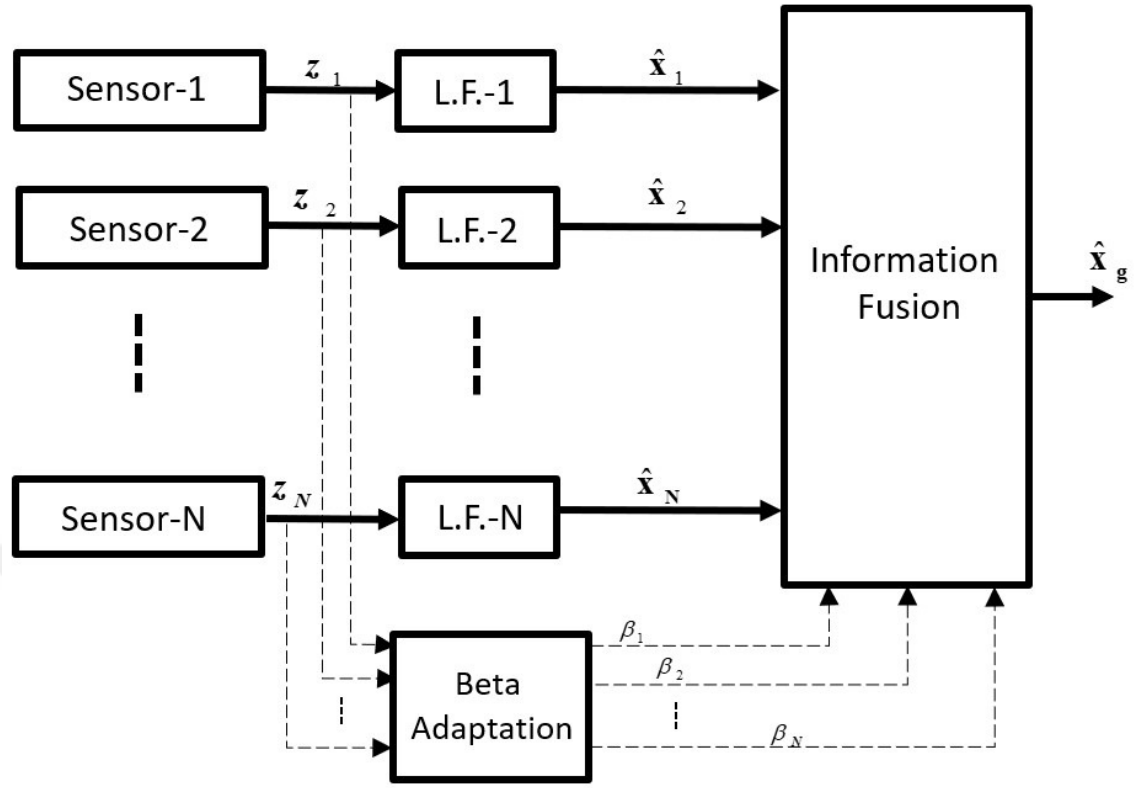


**Figure 4.4** No-Reset adaptive federated Kalman filter

based on RSSI readings and distance information gathered from RSSI readings for adaptive assignment of the information-sharing coefficients.

We used the distance-based lateration method among indoor positioning methods given in Figure 2.1 and assume that RSSI information is gathered from $N$ access points. To increase reliability of lateration results, the position data are obtained by multi-lateration via a set of $N-1$ APs around the target. That means, each multi-lateration set will not take into account only one of the RSSI readings. Let us denote the received power from the $j$-th AP as $P_{rj}$ and, according to (2.13), the distance that corresponds to this signal power as $d_j$. Also, consider three predetermined values $\beta_l$, $\beta_m$ and $\beta_h$ so that $0 < \beta_l < \beta_m < \beta_h < 1$ and

$$\beta_l + (N-2)\beta_m + \beta_h = 1. \tag{4.15}$$

To assign these values as the information sharing coefficients, we propose two methods, , namely, using an adaptation based on RSSI quality or on distance.

### 4.5.1 Adaptation based on RSSI quality

RSSI value of an AP is inversely proportional to the distance. Hence, it is expected to get RSSI with lowest power from farthest AP and highest power from closest one. First method is based on this rule. Let

$$q = \arg\min_{1 \leq j \leq N} \{P_{rj}\} \tag{4.16}$$

$$r = \arg\max_{1 \leq j \leq N} \{P_{rj}\} \tag{4.17}$$

In other words, $q$-th AP provides signal with worst quality and the best signal quality is received from the $r$-th one. After getting closest and farthest APs from signal power level, the information sharing coefficients $\beta_i$ $(i = 1, \ldots, N)$ are assigned as follows:

> If $z_i$ is a location measurement based on $\{P_{rj}\}_{j \neq q}$, then $\beta_i = \beta_h$.
> Else if $z_i$ is a location measurement based on $\{P_{rj}\}_{j \neq r}$, then $\beta_i = \beta_l$.
> Else $\beta_i = \beta_m$.

In other words, the information sharing coefficient of a location measurement that is obtained by excluding the highest received power, is assigned with the lowest value $(\beta_l)$ and the coefficient of the one that is obtained by excluding the lowest RSSI is set to the highest value $(\beta_h)$. The outputs of other local filters are weighted equally so as to satisfy (4.2).

### 4.5.2 Adaptation based on distance

One can get distance of the APs by using RSSI measurements via (2.13). Then, an alternative adaptation method is proposed in terms of the calculated distances of the APs. Similar to (4.16) and (4.17), let us consider

$$u = \arg\max_{1 \leq j \leq N} \{d_j\} \tag{4.18}$$

$$v = \arg\min_{1 \leq j \leq N} \{d_j\} \tag{4.19}$$

Note that the APs that appear closest and farthest may differ from those that give the lowest and highest RSSI readings, respectively, since the estimated values of the parameters $X_\sigma$ and $n_p$ via (2.18), which are used in (2.13) to calculate distance may differ among the APs. The information-sharing coefficients of the federated Kalman filter will be assigned as:

If $z_i$ is multi-laterated from $\{d_j\}_{j\neq u}$, then $\beta_i = \beta_h$.
Else if $z_i$ is multi-laterated from $\{d_j\}_{j\neq v}$, then $\beta_i = \beta_l$.
Else $\beta_i = \beta_m$.

The $\beta_l$, $\beta_m$ and $\beta_m$ coefficients can be chosen by considering the expected noise levels of the access points. For the case of four access points, it is possible to get four tri-lateration solutions. If one of these tri-laterated solution is very poor and rest of the results are relatively better (that means the signals from three AP are more noisy than the other less noisy one), one can prefer to assign smaller and closer values to $\beta_l$ and $\beta_m$, and define $\beta_h$, higher. At another case one of the APs may not be able good results with respect to other three APs. Then, it might be better to choose $\beta_l$ as small as possible and give closer weights to $\beta_m$, $\beta_h$.

## 4.6 Adaptation of Information Sharing Coefficients with FKF-SCU structure

At the FKF-SCU structure detailed in section 4.4 there is not an information sharing mechanism and equal information sharing strategy is applied for no-faulty situation. In this section, another indoor localization method is proposed with combination of FKF-SCU structure and information sharing coefficient adaption. For normal operation of the system, information sharing coefficient adaptation is applied either considering RSSI quality or distance information as given in Section 4.5. Whenever a fault is detected, at that faulty step covariance update skipping is applied and information coefficients are set to a minimum value regarding to the combination of laterations including faulty AP. Hence, we can say that information sharing coeffi-

cients are adaptive throughout the whole process like in Section 4.5, and additionally, there will be a tolerance to sensor faults. The complete algorithm that uses combination of adaptive information sharing coefficients with FKF-SCU is represented in Figure 4.5.

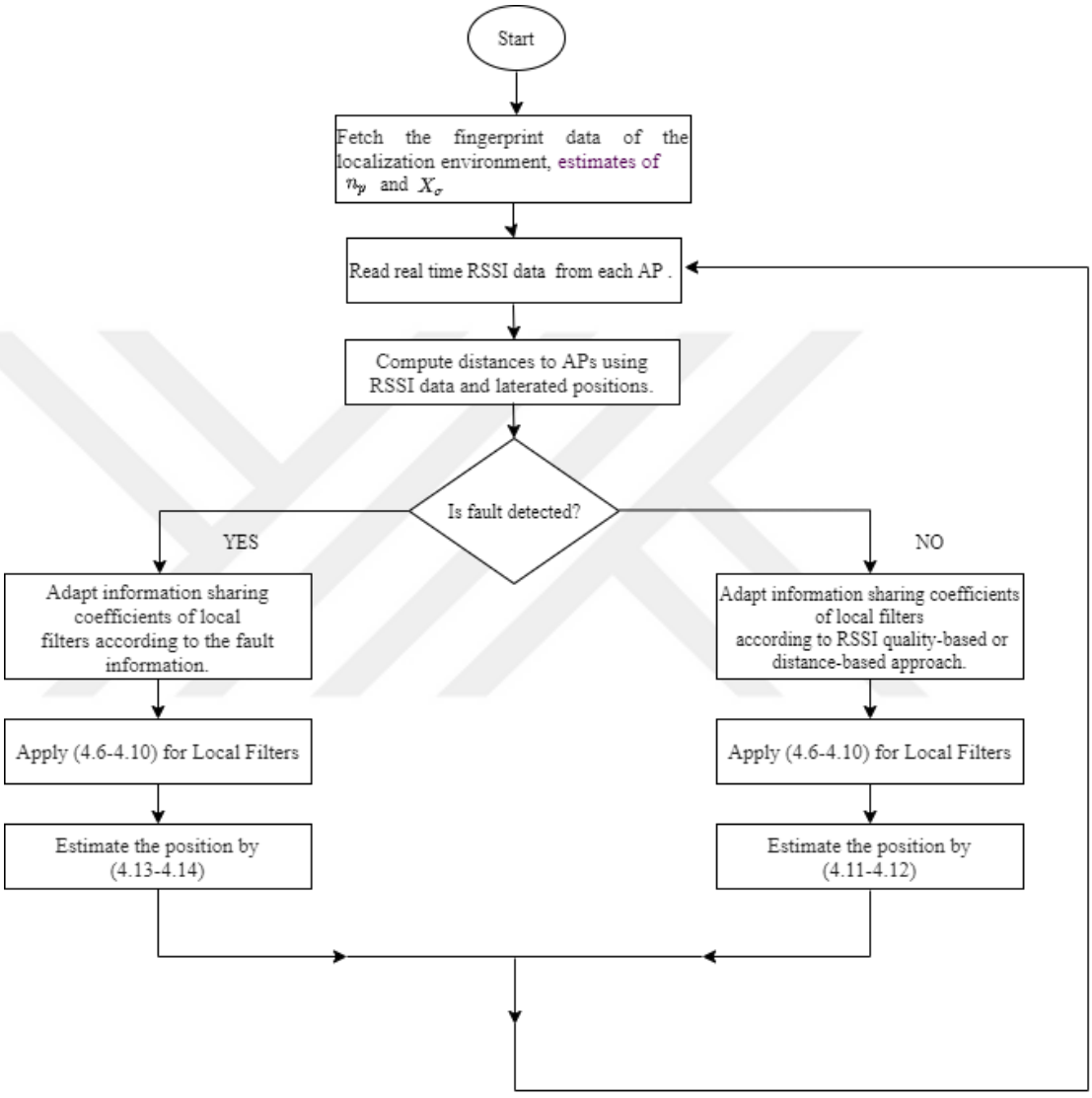


**Figure 4.5** Fault tolerant positioning algorithm with adaptive FKF-SCU

## 4.7 Conclusions

In this chapter, localization methods used for indoor environment are shown. CKF and FKF are regular methods for outdoor positioning applications and these regular methods are applied for indoor positioning in this study. New methods for fault tolerant and adaptive indoor positioninge are also given. These methods are

based on FKF and take place main contribution of the study. As first contribution skipped covariance update structure is proposed with motivation of the fault tolerant structure of FKF. Secondly, more important contribution as online adaptation methods for information sharing coefficients are proposed. Lastly these two new structures are combined for an adaptive fault tolerant positioning method. At next chapter simulations are performed with these methods by using both synthetic and real environment data.

# 5. TEST AND SIMULATION RESULTS

In order to test performance of sensor fusion methods given above, simulations are performed both with generated synthetic data and collected real environment data. Initially performances of CKF, FKF and Single Kalman Filter (SKF) are compared in scope of multi-sensor positioning. After that real data is collected at two different locations. Faulty situation is also considered to not only asses positioning accuracy but also fault tolerance performances. Then different methods are performed and results are discussed. For all simulations the dynamic model of a target moving on a two-dimensional coordinate space with a constant velocity is used [70].It is also assumed that the velocity of the model is updated via the information gathered from inertial sensors of the target device. Let us denote the $x$-coordinates of the position and the velocity of the target at instant $k$ as $p_x(k)$ and $v_x(k)$, respectively. whereas the $y$-coordinates of its position and velocity are $p_y(k)$ and $v_y(k)$.

$$\begin{bmatrix} p_x(k) \\ v_x(k) \\ p_y(k) \\ v_y(k) \end{bmatrix} = \begin{bmatrix} 1 & 1 & 0 & 0 \\ 0 & 1 & 0 & 0 \\ 0 & 0 & 1 & 1 \\ 0 & 0 & 0 & 1 \end{bmatrix} \begin{bmatrix} p_x(k-1) \\ v_x(k-1) \\ p_y(k-1) \\ v_y(k-1) \end{bmatrix} + \begin{bmatrix} w_{p,x}(k) \\ w_{v,x}(k) \\ w_{p,y}(k) \\ w_{v,y}(k) \end{bmatrix} \tag{5.1}$$

$$\begin{bmatrix} p_x(k) \\ p_y(k) \end{bmatrix} = \begin{bmatrix} 1 & 0 & 0 & 0 \\ 0 & 0 & 1 & 0 \end{bmatrix} \begin{bmatrix} p_x(k) \\ v_x(k) \\ p_y(k) \\ v_y(k) \end{bmatrix} + \begin{bmatrix} v_{p,x}(k) \\ v_{p,y}(k) \end{bmatrix} \tag{5.2}$$

For all simulations, the output is the position of the target that is tracked with known initial position and for different sections of the trajectory, similar models are used. There are many different methods to find the position of the target in an indoor environment as described in Section 2. In this study, we get the location information from lateration calculations. Note that we need to know distances between target

and APs to apply the lateration method to obtain the position data of the target. When more than three sensors are used it is called multi-lateration, and if there are three sources it is called tri-lateration as shown in Figure 2.2. The distances used for lateration are calculated via RSSI measurements which is a measure of RF energy received at the target. Note that, in general, if data is available from $n$ APs, they can be $r$-laterated in

$$C(n,r) = \frac{n!}{r!(n-r)!} \tag{5.3}$$

different ways, where $C$ denotes combinations. In our simulations we used four APs. Since four RSSI are readings are available at each measurement point, $C(4,3) = 4$ combinations of them are available for tri-laterations. Then, the position values obtained as the result of these tri-laterations can be used as inputs to federated or centralized Kalman filters.

## 5.1 Simulations with generated data

Data generation for simulations is started with defining the indoor area dimensions and locations of APs. In our model, we have four different access points located at $[0, 10; 0, 0; 15, 0; 15, 10]$. To get more realistic data in order to asses performance of FKF first of all actual distances of target from APs are calculated and then from these distance informations actual RSSI values are gathered. After that additive white gaussian noises with three different levels $X_\sigma = 1, 2, 3$ dBm are generated so as to simulate disturbances acting on RSSI measurements and added to actual RSSI values by using the propagation model shown below

$$P_r = P_0 - 10n_p \log(d) + X_\sigma \tag{5.4}$$

One can compute the distance between the target and an AP as

$$d = 10^{(P_0 - P_r + X_\sigma)/(10n_p)} \tag{5.5}$$

and all parameters must be known for distance calculation. Here, $P_0$ values are used as $-52.75$, $-57.69$, $-56.93$, $-58.96$, respectively, for each AP and the path loss exponent $n_p$ is taken as 2.18 [18].

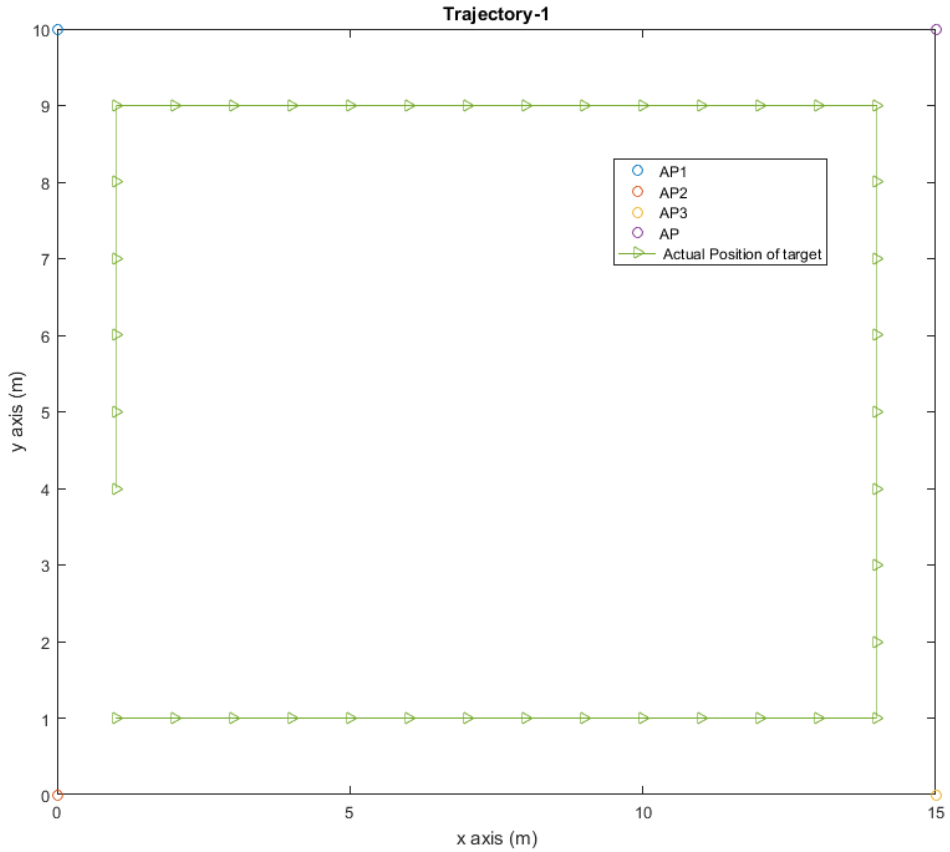


**Figure 5.1** Position of access points & target movement for Trajectory-1

Assuming that we get only one position information, SKF simulations are performed with first three AP's trilateration measurements and lowest measurement noise. All results are recorded considering both $x$ and $y$ axis and shown at Table 5.1. When we compare the results, SKF shows worser performance than both FKF and CKF at all axes with all noise levels. On the other hand, CKF and FKF provides similar results as expected regarding to federated filter theory proposed in [32].

Table 5.2 shows us the results of the second trajectory. MSE values given here are not calculated considering full trajectory, since the trajectory is rather challenging. Values are calculated for defined intervals which are given in parentheses. Comparing the results for the second trajectory, it is seen that the performances of FKF and CKF are similar. But, SKF performs better than the other filters in some intervals.

**Table 5.1** MSE values of position estimates (m) for trajectory-1 with $X_\sigma = 1, 2, 3dBm$

| dBm | Axis | SKF | CKF | FKF | LF1 | LF2 | LF3 | LF4 |
|---|---|---|---|---|---|---|---|---|
| 1 | $X$ | 1.1936 | 0.7485 | 0.7442 | 1.6529 | 1.3414 | 1.2444 | 1.1792 |
| | $Y$ | 2.5698 | 1.8496 | 1.8034 | 3.7864 | 3.0642 | 2.6147 | 2.3999 |
| 2 | $X$ | 2.4453 | 1.5970 | 1.5867 | 3.4965 | 2.8885 | 2.6364 | 2.4014 |
| | $Y$ | 5.4945 | 3.9623 | 3.8545 | 8.1113 | 6.5714 | 5.3617 | 5.0626 |
| 3 | $X$ | 3.8562 | 2.5101 | 2.4912 | 5.6048 | 4.5846 | 4.1622 | 3.7555 |
| | $Y$ | 8.7517 | 6.3529 | 6.1828 | 13.0518 | 10.5327 | 8.6538 | 8.1211 |

After many simulations, considering FKF and SKF performances it is inferred that fusing more than one information provides better result. As stated before FKF is known with its fault tolerant performance. Hence faulty scenario is generated so as to asses FKF performance for faulty situations. To assess fault tolerance performance of the system a scenario is generated at second trajectory and blunders are applied directly to the position information calculated by trilateration. Another faulty scenario is created by assigning zero dBm values at some instants, assuming that there is no information from APs because of a voltage problem or shut-down status, etc. Then, positioning system cannot get information from APs for localization. During these scenarios 1 $dBm$ and 3 $dBm$ $X_\sigma$ are also used to generate more realistic simulations. As a disturbance effect 2 m positioning information is added 5th and 15th steps of trajectory and 25-29th step is fixed to 0 m. The results for this scenario are given in Table 5.3. MSE values are calculated with information for two steps after occurrence/end of blunders. Hence, we take in consideration the values of the steps between $6-8$, $16-18$ and $30-32$ to make a decision for the fault tolerant performance of filters.

Table 5.3 shows us a summary of simulation results for faulty situation. This table clearly show us, while applying faults all three different type of filters performance degrades. Results are calculated considering the intervals given in parenthesis and performance of CKF and FKF are again similar, as expected from the federated

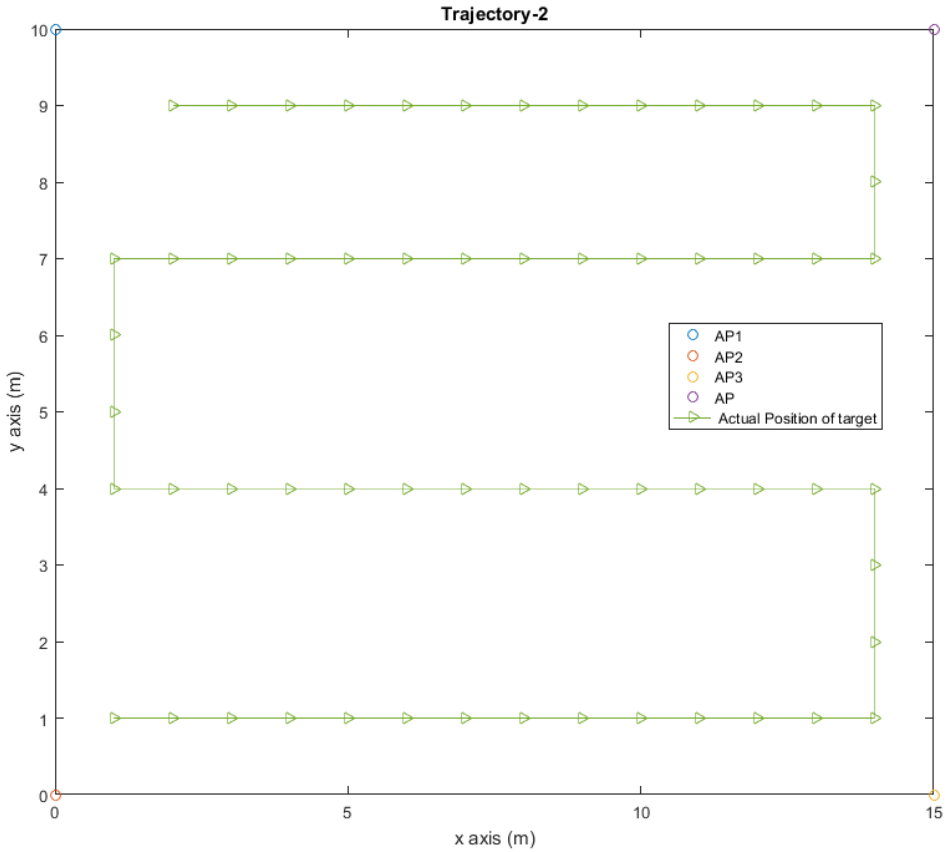


**Figure 5.2** Position of access points  target movement for Trajectory-2

filter theory [32]. General performance of SKF simulations seems closer to FKF and CKF but it shows worser performance than other filters except in two intervals, that is, $x(6-8)$ and $y(30-32)$. Performance of FKF may not be satisfactory when we take fault tolerance into consideration. But, it must be emphasized that we kept information-sharing coefficients identical for local filters throughout the simulations.

## 5.2 Test Set-up for Real Data Collection

Simulations performed with the generated data provided promising results about performance of multi-sensor fusion structure for indoor positioning. Then, to extend the study using real-environment data and test the indoor performances of centralized and federated filtering techniques, measurement data is collected and

**Table 5.2** MSE values of position estimates (m) for trajectory-2 with $X_\sigma = 1, 2, 3dBm$

| dBm | Filter Type | X (15-24) | X (31-40) | X (46-55) | Y (15-24) | Y (31-40) | Y (46-55) |
|---|---|---|---|---|---|---|---|
| 1 | $SKF$ | 1.0952 | 1.3907 | 1.8340 | 3.6808 | 0.4221 | 3.9423 |
| | $CKF$ | 0.6969 | 0.7493 | 0.9052 | 2.249 | 0.5741 | 2.4720 |
| | $FKF$ | 0.7190 | 0.7375 | 0.9115 | 2.113 | 0.6341 | 2.3334 |
| 2 | $SKF$ | 2.0092 | 2.6481 | 3.5225 | 7.5605 | 0.8419 | 8.2142 |
| | $CKF$ | 1.3344 | 1.4841 | 1.8529 | 4.5262 | 1.2338 | 5.3733 |
| | $FKF$ | 1.3570 | 1.4868 | 1.8389 | 4.2648 | 1.3410 | 5.0768 |
| 3 | $SKF$ | 2.8766 | 4.0233 | 5.7905 | 11.2447 | 1.3150 | 13.8878 |
| | $CKF$ | 2.0588 | 2.3411 | 2.9609 | 7.4064 | 1.9110 | 8.7648 |
| | $FKF$ | 2.0832 | 2.3320 | 2.9170 | 6.9232 | 2.0853 | 8.2800 |

RSSI measurements are stored via NetSurveyor program running on a Lenovo Ideapad FLEX 4 laptop, which has an Intel Dual Band Wireless-AC 8260 Wi-Fi adaptor.

Measurements are collected in two different-sized test beds in indoor areas which are denoted as TB1 and TB2 below. Size of first test bed (TB1) is 20 $m^2$ are (4 m $\times$ 5 m and size of second test bed (TB2) is 46.77 $m^2$ (4.95 m $\times$ 9.45m). These test beds were set up at Kadir Has University, Istanbul, Turkey. Wireless access points are located at corners of the test bed and markers are placed at every 50 cm and 45 cm in TB1 and TB2 respectively. Measurements are carried out on the grid shown in Figures 5.3 and 5.4 and collected data is provided at [71, 72].

**Table 5.3** MSE values of position estimates (m) for faulty situation $X_\sigma = 1, 3dBm$

| dBm | Filter Type | X (6-8) | X (16-18) | X (30-32) | Y (6-8) | Y (16-18) | Y (30-32) |
|---|---|---|---|---|---|---|---|
| 1 | $SKF$ | 0.2952 | 1.1905 | 2.1111 | 5.3371 | 1.4968 | 0.4728 |
| | $CKF$ | 0.3792 | 0.9976 | 1.3265 | 3.3175 | 0.9774 | 0.7387 |
| | $FKF$ | 0.3832 | 1.028 | 1.3446 | 3.1178 | 0.9954 | 0.7824 |
| 3 | $SKF$ | 0.7336 | 3.6937 | 5.022 | 17.1248 | 4.8783 | 0.6586 |
| | $CKF$ | 1.0942 | 3.0999 | 3.5976 | 10.7145 | 3.2371 | 2.2109 |
| | $FKF$ | 1.1295 | 3.2508 | 3.625 | 10.1594 | 3.2507 | 2.4841 |

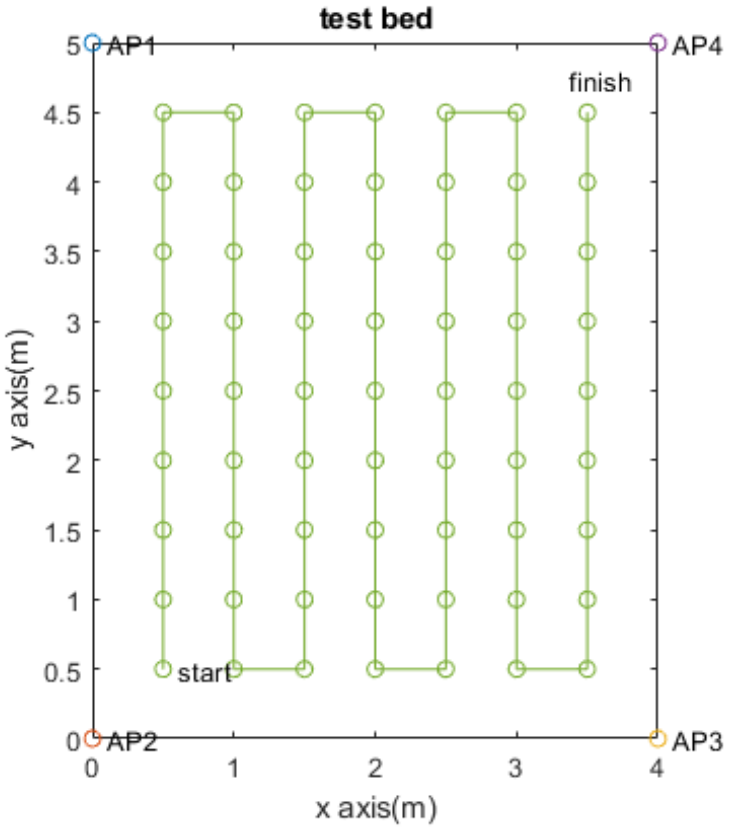


**Figure 5.3** TB1 and measurement points

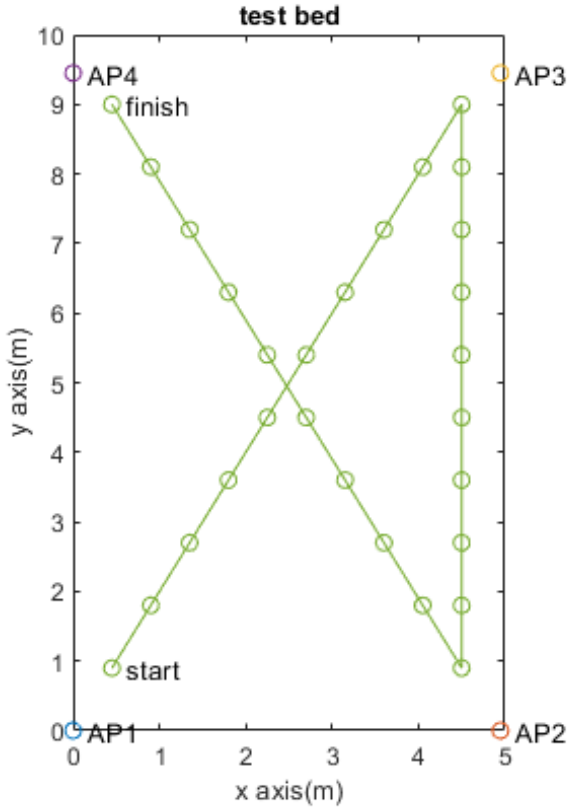


**Figure 5.4** TB2 and measurement points

At each measurement point, RSSI data is collected for 1 min with a sampling interval of 250 ms. This collected data is divided in two parts so that 50% is used as training data and 50% as test data. While training data is used for parameter calculations, simulations are performed with test data. Collected RSSI measurements are shuffled in 50 different ways to avoid any bias due to the selection of training data.

Collected training data is also compared with RSSI values gathered via estimated model at each measurement point. Initially, parameters of the environment are estimated with (2.18) and known real distances of measurement points for each AP. After that estimated RSSI values are calculated with (2.12). Change of RSSI power level with respect to distance is shown in Figures 5.5 and 5.6. Due to propagation nature of radio signals, power of RSSI decreases when the target move away from

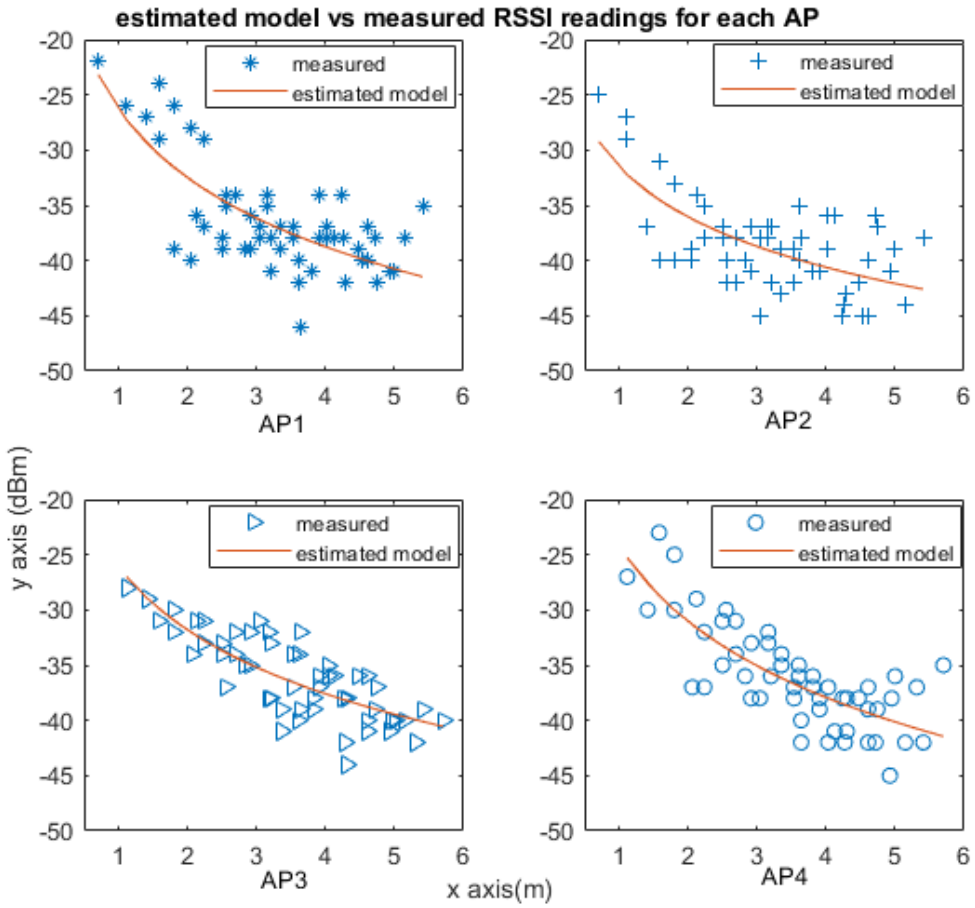


**Figure 5.5** RSSI measurements for TB1

the AP. The quality of signal increases when the distance between target and AP decreases.

In each case, anomalies at test data with respect to training data can be detected by comparing the maximum of RSSI values of the test data to the minimum of the fingerprint data. Alternatively, one can monitor a deviation (predefined in terms of the standard deviation of the training RSSI data, $\sigma$) from its mean. In this study, we used $1\sigma$ and $3\sigma$ thresholds for detecting the faulty APs. All results given below are averaged values of 50 simulation runs.

In Chapter 2, reliability of RSSI data to be used for positioning purposes is mentioned. To support this issue, position information are calculated via tri-lateration

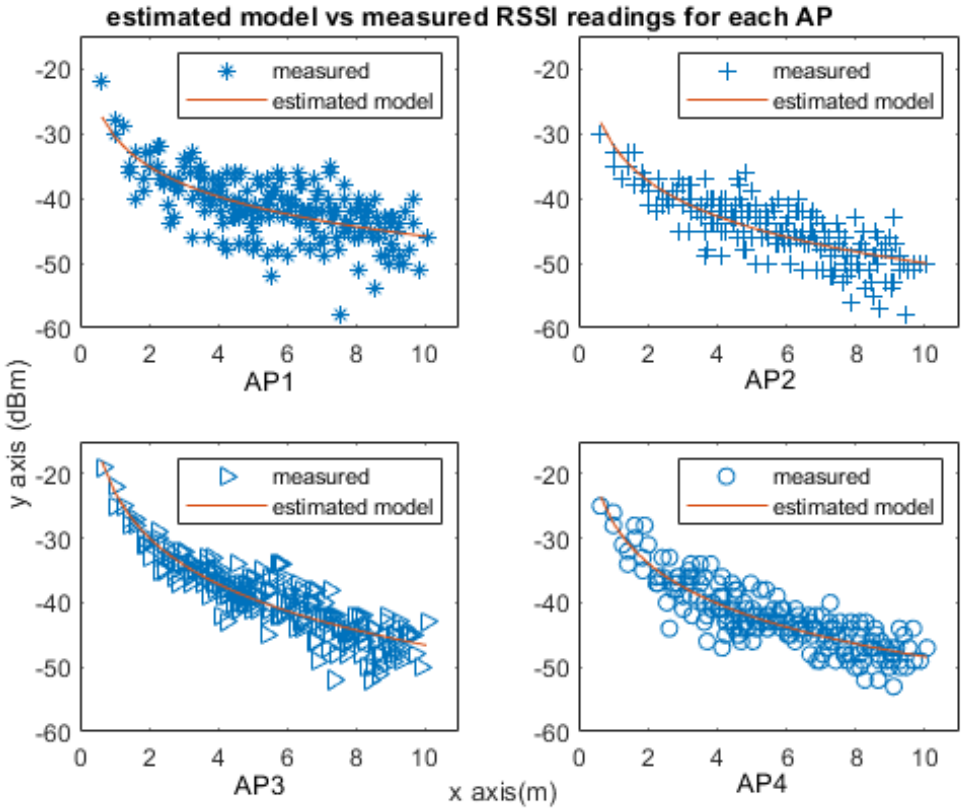


**Figure 5.6** RSSI measurements for TB2

and multi-lateration considering all measurements of TB1 and TB2. The averaged mean square error performances are given at Table 5.4, where 'Trilat$(i, j, k)$' denotes a tri-lateration based on three access points labeled as $i$, $j$, $k$ and 'Multilat' stands for a lateration that uses the data from all four APs. Even the lowest error for tri-laterations (1.78 m and 3.45m for AP's 1, 3 and 4) is considerably large for an indoor environment.

**Table 5.4** Average Mean-Square Errors in Lateration Positioning (meters)

| | **Multilat** | **Trilat(1,2,3)** | **Trilat(1,2,4)** | **Trilat(1,3,4)** | **Trilat(2,3,4)** |
|---|---|---|---|---|---|
| TB1 | 1.62 | 2.57 | 2.11 | 1.78 | 2.43 |
| TB2 | 3.87 | 5.29 | 5.36 | 3.45 | 3.61 |

Moreover, in order to analyze how RSSI data varies in indoor environment, more than 50 values are collected for each AP from one meter distance. Figure 5.2 shows minimum, maximum and average values for each AP. A histogram of RSSI values is given in Figure 5.2, which depicts the distribution of 1m-RSSI measurements. Average of all 1m measurements, which is plotted in Figure 5.2 is $-33.1835$ dBm and the RSSI values lay around $-30$ dBm. As a result, lateration positioning errors and distribution of RSSI values show us that we cannot trust RSSI results without processing them.

The dynamic model of the target moving on a two dimensional space with a constant velocity is used again for real data simulations [70] whose system and measurement equations are given by (5.1) and (5.2).

The process and measurement noise matrices that are obtained by simulation and used for all simulations are

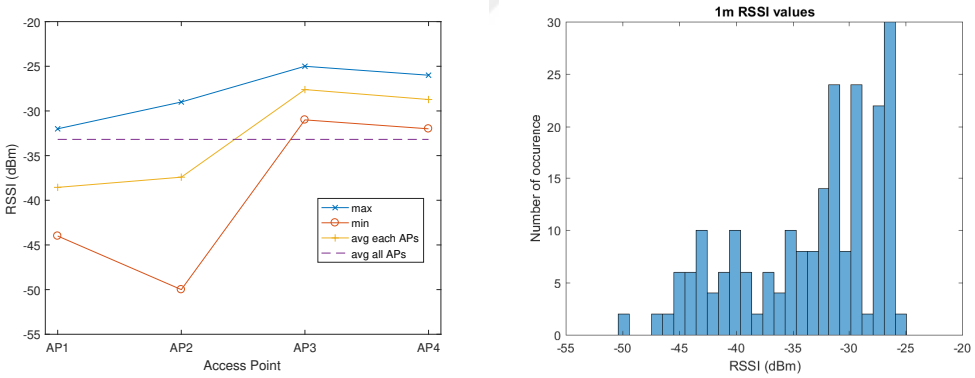


(a) Minimum and maximum values (b) Histogram

**Figure 5.7** RSSI measurements at 1m distance from the APs

$$\mathbf{Q}_1 = \begin{bmatrix} 0.005 & 0 & 0 & 0 \\ 0 & 0.0005 & 0 & 0 \\ 0 & 0 & 0.0005 & 0 \\ 0 & 0 & 0 & 0.005 \end{bmatrix} \tag{5.6}$$

$$\mathbf{Q}_2 = \begin{bmatrix} 0.005 & 0 & 0 & 0 \\ 0 & 0.0001 & 0 & 0 \\ 0 & 0 & 0.005 & 0 \\ 0 & 0 & 0 & 0.0001 \end{bmatrix} \tag{5.7}$$

and

$$\mathbf{R}_1 = \begin{bmatrix} 4 & 0 \\ 0 & 4 \end{bmatrix} \tag{5.8}$$

$$\mathbf{R}_2 = \begin{bmatrix} 16 & 0 \\ 0 & 16 \end{bmatrix} \tag{5.9}$$

To convert RSSI values to distances to get range from the access points, the parameters $P_0$,$n_p$ an $X_\sigma$ in (2.13) must be determined.

The reference signal power $P_0$ of each AP are gathered by taking the average of 50 measurements collected at 1m distance from each AP. Reference signal power values of each AP are shown in Table 5.5. Other two parameters, the path loss exponent and the fading parameter are estimated using (2.18). To estimate these parameters, received signal is used and power with the highest RSSI values of collected data at each measurement point in the training data is chosen for estimation.Estimated parameters are shown in Table 5.6.

**Table 5.5** Reference Signal Powers (dBm)

| | **AP 1** | **AP 2** | **AP 3** | **AP 4** |
|---|---|---|---|---|
| TB1 | −39.71 | −35.32 | −31.02 | −34.05 |
| TB2 | −33.76 | −38.00 | −27.61 | −28.72 |

**Table 5.6** Path Loss Exponents and Fading Parameters

| | | **AP 1** | **AP 2** | **AP 3** | **AP 4** |
|---|---|---|---|---|---|
| TB1 | $n_p$ | 2.11 | 1.46 | 1.56 | 1.96 |
| | $X_\sigma$ | 12.65 | 10.79 | 12.70 | 2.11 |
| TB2 | $n_p$ | 1.54 | 1.83 | 2.37 | 2.09 |
| | $X_\sigma$ | 8.21 | 10.54 | 18.49 | 1.22 |

## 5.3 Fault Tolerant Positioning Algorithm and Test Results

After collecting RSSI measurements at two different test beds, simulations are performed with FKF and CKF for no-fault and faulty situation. Moreover FKF-SCU performance is also evaluated for faulty situation. These three cases are described below.

1. *CKF and FKF (no-fault scenario)*: In first case collected raw data is used for the simulations with FKF and CKF. Equal information sharing coefficients are chosen for FKF structure and they are kept constant for whole process. Equal coefficients mean in other words, all local estimates contribute to the global estimate equally ($\beta_i = 1/4$ for $i = 1, \dots 4$). Afterwards FKF and CKF are applied without any change at their structure as described in (4.3)–(4.12) and (3.6)–(3.10) respectively.
2. *CKF and FKF (fault scenario)*: In second case fault scenario is created different from first case. As faulty scenario, it is assumed that AP1 is shut down for five seconds. Therefore RSSI data cannot be gathered for five consecutive measurement steps. Again equal information sharing coefficients are chosen for FKF, there is no change at FKF and CKF structure that are used for localization as in case 1.

3. *FKF-SCU (fault scenario)*: In the last case,fault scenario described in second case is applied. Whenever a fault is detected at one of the APs, information fusion is carried out using (4.13) and (4.14) as described in Section 4.4. Moreover, information sharing coefficients are initialized with equal values but at faulty steps the information sharing coefficients of the LFs processing the trilaterations involving the faulty AP are set to a minimum, i.e., very close to zero. So, considering the resetting step (4.3) and proposed skipping step (4.14) in FKF-SCU structure, the LF estimates, which process this faulty measurement are not effective in the global estimate computation at the information fusing stage.

Position estimation performances of CKF and FKF filters for the first case in which there is no faulty situation are given in Table 5.7.For TB1, an average MSE error below $1m$ is achieved for both filtering structures. On the other hand in TB2, because of the increased distance between APs and general area of the indoor environment, average MSE error also increased which is below $2m$ for both filtering structures. Due to equal information sharing and resetting mode of FKF,simulation results for CKF and FKF are equal as expected [69].

**Table 5.7** Average Mean Square Estimation Errors of CKF and FKF for the no-fault scenario (m)

| | **TB1** | | **TB2** | |
|---|---|---|---|---|
| | **CKF** | **FKF** | **CKF** | **FKF** |
| Minimum | 0.13 | 0.13 | 0.25 | 0.25 |
| Maximum | 2.21 | 2.21 | 7.39 | 7.39 |
| Average | 0.74 | 0.74 | 1.67 | 1.67 |

In the second case CKF and FKF structures remain same as in first case. But, for this case a signal loss scenario created as faulty situation and it is assumed that the signal is not obtained from AP1 between the 13th and 17th steps (totally five seconds, which means five steps). At signal loss steps RSSI measurements are recorded as $-100$dBm for computational purposes. Simulation results of this case

are shown in Table 5.8 and estimation errors is shown in Figure 5.8 for TB1 and TB2. Effect of the fault can be clearly seen in Figure 5.8. With the beginning of faulty step the estimation errors of FKF and CKF increase to a magnitude of $10^5$m. Moreover the errors stay above $10^4$m for a long period of time after the faulty AP starts its normal operation. In TB2 estimation error increase to a magnitude of $10^7$m. Even the error behaviour of TB2 is worse than TB1, it can be deduced from the results that none of the filtering structure can recover the system output in case of a faulty situation.

**Table 5.8** Average Mean Square Estimation errors of CKF and FKF for the fault scenario (m)

| | **TB1** | | **TB2** | |
|---|---|---|---|---|
| | **CKF** | **FKF** | **CKF** | **FKF** |
| Minimum | 0.29 | 0.29 | 1.22 | 1.22 |
| Maximum | $7.66 \cdot 10^5$ | $7.66 \cdot 10^5$ | $6.97 \cdot 10^7$ | $6.97 \cdot 10^7$ |
| Average | $1.16 \cdot 10^5$ | $1.16 \cdot 10^5$ | $2.05 \cdot 10^7$ | $2.05 \cdot 10^7$ |

In the last case, simulations are performed in a fault scenario as described in second case. A detection rule is proposed to detect faults and FKF-SCU algorithm is applied as detailed in Section-4.4. Training data that refers to 50% of the RSSI measurements are accepted as the fingerprint data which means that it is nominal measurements of the test environment. Remaining 50% of the RSSI measurements are kept as test data and it is used as measurement information input to estimate location of the target. In order to detect occurrence of a possible faulty and identify the faulty access point, test data is compared with the environmental fingerprint data at each step. Comparison of the test data and the fingerprint data is performed according to the following fault detection rule:

**Detection rule:** If the difference between the mean of the fingerprint data and the maximum RSSI value of any access point is larger than the detection threshold, then declare this AP as faulty.

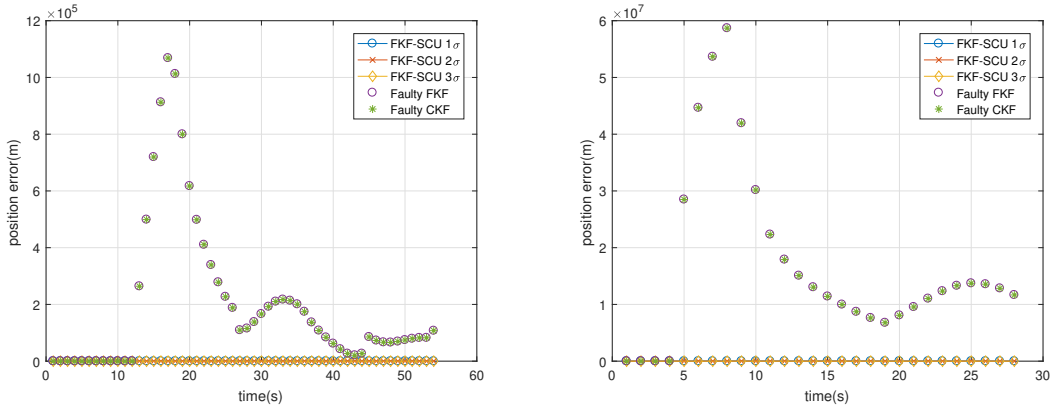


(a) Test Bed 1 (b) Test Bed 2

**Figure 5.8** CKF and FKF estimation errors

As it is seen at detection rule, we need to have statistical data of fingerprint data to use that rule. Hence standard deviation and mean values of fingerprint data are also stored so as to apply detection rule. Since received power deviates at each point, among test data only maximum RSSI values which means the best received power of each point are considered.

When we have a look at the performance of the FKF-SCU in Figure 5.8-5.9, drastic improvement can be easily seen. Estimation error performances gathered with FKF-SCU simulations are shown in Table 5.9 for three different detection thresholds, namely, $1\sigma$, $2\sigma$ and $3\sigma$. It is obvious that even applying the faulty scenario the FKF-SCU provides similar performance to the no-fault scenario at both two test beds. Performances of different thresholds are similar with slight differences. Since covariance update is skipped more frequently when smaller thresholds are chosen and more RSSI values are likely to be classified as faulty, lowest threshold $1\sigma$ performs a bit worse with respect to the highest threshold $3\sigma$. As a result, the average estimation error also increases. Even though there is small differences between the performances, the relevance of choice for the detection threshold and distances between APs can be seen in Table 5.9. Estimation error performance for TB1 is around $0.75m$ and smaller than $1m$. In TB2 estimation error is around $1.68m$ and smaller than $2m$ with proposed method, whereas in [18] an average error of $1.3m$ is achieved for indoor environment with $6mx6m$ dimensions and average errors not

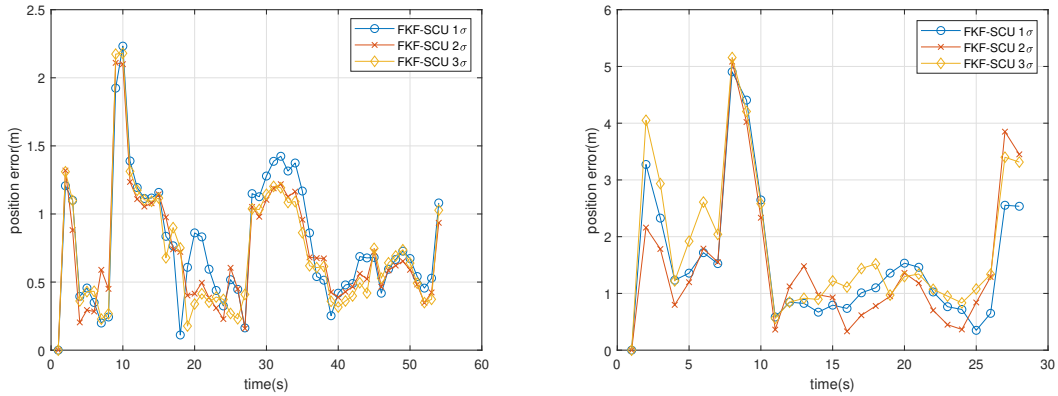


(a) Test Bed 1 (b) Test Bed 2

**Figure 5.9** FKF-SCU estimation errors

less than $1.6m$ are obtained by the teams, which competed in the infrastructure-free category in [17].

**Table 5.9** Average Mean Square Estimation errors of FKF-SCU for fault scenario (m)

| | **TB1** | | | **TB2** | | |
|---|---|---|---|---|---|---|
| | $1\sigma$ | $2\sigma$ | $3\sigma$ | $1\sigma$ | $2\sigma$ | $3\sigma$ |
| Minimum | 0.14 | 0.13 | 0.14 | 0.31 | 0.29 | 0.29 |
| Maximum | 2.23 | 2.11 | 2.18 | 4.91 | 5.08 | 5.15 |
| Average | 0.76 | 0.74 | 0.73 | 1.68 | 1.67 | 1.68 |

It can be understood from these results that whenever RSSI measurements cannot be gathered from an access point, estimation performance can be substantially enhanced by adapting the filter parameters. At this point another issue is to have the RSSI fingerprint data of the target localization environment to define and apply a fault detection rule.

The cumulative distribution functions (CDF) of the average estimation error for three cases are shown at Figure 5.10. For TB1, the error is low, i.e. below 1m during 75% of the time with similar results for all scenarios. On the other hand, the estimation error in TB2 is higher than the results gathered in TB1. In TB2 estimation errors rise to 2 m and 2.4 m 75% of the time under no-fault and fault

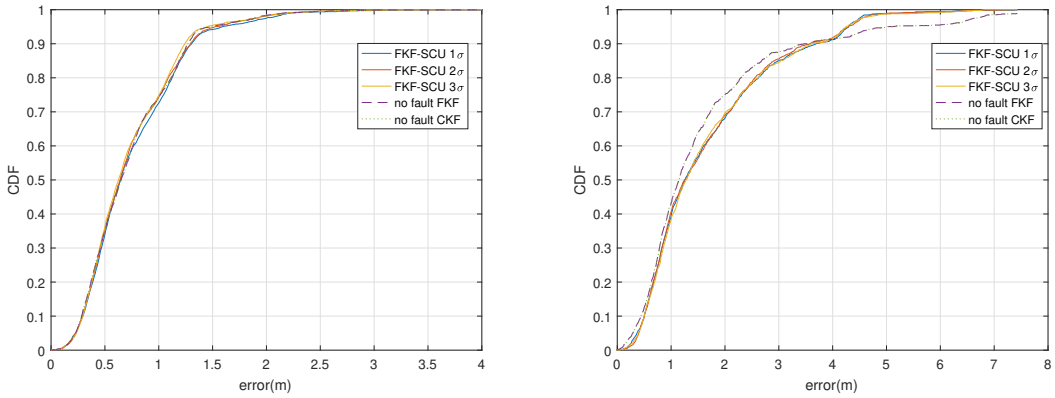


(a) Test Bed 1 (b) Test Bed 2

**Figure 5.10** Cumulative distribution function of estimation errors

conditions, respectively. However, the error in TB2 is below 1 m around 40% of the time for no-fault and fault cases. TB1 and TB2 are two different indoor locations with different dimensions and ranges between APS. Main reason of the performance difference between the test beds is that due to RF nature of RSSI propagation, the RSSI values drastically decrease as the distance between the target and the APs increases. For second case, since average estimation errors of CKF and FKF is around $10^5$m as shown above, the CDFs corresponding to these cases are omitted.

## 5.4 Simulations with Adaptation of Information Sharing Coefficients and Test Results

At first simulations a faulty scenario is generated and performance of CKF,FKF and proposed FKF-SCU is compared. During these simulations information sharing coefficients of FKF and FKF-SCU are chosen equal. Hence effect of different information sharing coefficients is not fully assessed yet. For this purpose two adaptation method described in Section 4.5 is applied for the collected data in TB2. Average estimation errors for different information sharing coefficients used with the two adaptation approaches in FKF-No reset structure are given in Tables 5.10-5.12. The equal sharing of information sharing coefficients ($\beta_i = 0.25$ for $i = 1, \ldots, 4$) refers to no-adaptation case and its performance is compared with the performance of adaptive coefficients. The performance difference between adaptive and non-adaptive FKF is evaluated

in terms of percentage to give a clear understanding of performance enhancement provided by online information sharing adjustment. Different information sharing coefficient sets are used during simulations and results of three of them are shown in Tables 5.10-5.12. It is clearly seen that all three set of adaptive coefficients provide performance improvement. When compared between each other increasing highest coefficient $\beta_h$ enhances the estimation error performance. These results show that online adjustment of the information-sharing coefficients can provide considerably higher estimation performance for a suitable selection of $\beta_h$, $\beta_m$ and $\beta_l$.

**Table 5.10** Average Mean-Square Errors (m) ($\beta_l = 0.1$, $\beta_m = 0.25$, $\beta_h = 0.4$)

| Adaptation | $\beta_i = 0.25\ \forall i$ | Adaptive FKF | **Improvement (%)** |
|---|---|---|---|
| RSSI-based | 1.70 | 1.69 | 0.53 |
| Distance-based | 1.70 | 1.63 | 3.67 |

**Table 5.11** Average Mean-Square Errors (m) ($\beta_l = 0.1$, $\beta_m = 0.15$, $\beta_h = 0.6$)

| Adaptation | $\beta_i = 0.25\ \forall i$ | Adaptive FKF | **Improvement (%)** |
|---|---|---|---|
| RSSI-based | 1.70 | 1.61 | 4.95 |
| Distance-based | 1.70 | 1.48 | 12.56 |

**Table 5.12** Average Mean-Square Errors (m) ($\beta_l = 0.05$, $\beta_m = 0.075$, $\beta_h = 0.8$)

| Adaptation | $\beta_i = 0.25\ \forall i$ | Adaptive FKF | **Improvement (%)** |
|---|---|---|---|
| RSSI-based | 1.70 | 1.48 | 12.68 |
| Distance-based | 1.70 | 1.39 | 18.29 |

As can be seen from Tables 5.10-5.12, simulations performed with the adaptive coefficients based on the distance between the target and APs provided better results than directly using the RSSI levels. Main reason for this performance difference is that the proximity of the target to APs inferred by using RSSI value can be adjusted by considering different propagation parameters for each APs.

The estimated cumulative distribution functions (CDF) of average estimation errors that are shown in Figures (5.11-5.13) for different information-sharing coefficient sets also proves the performance improvement provided by information sharing coefficient adaptation.

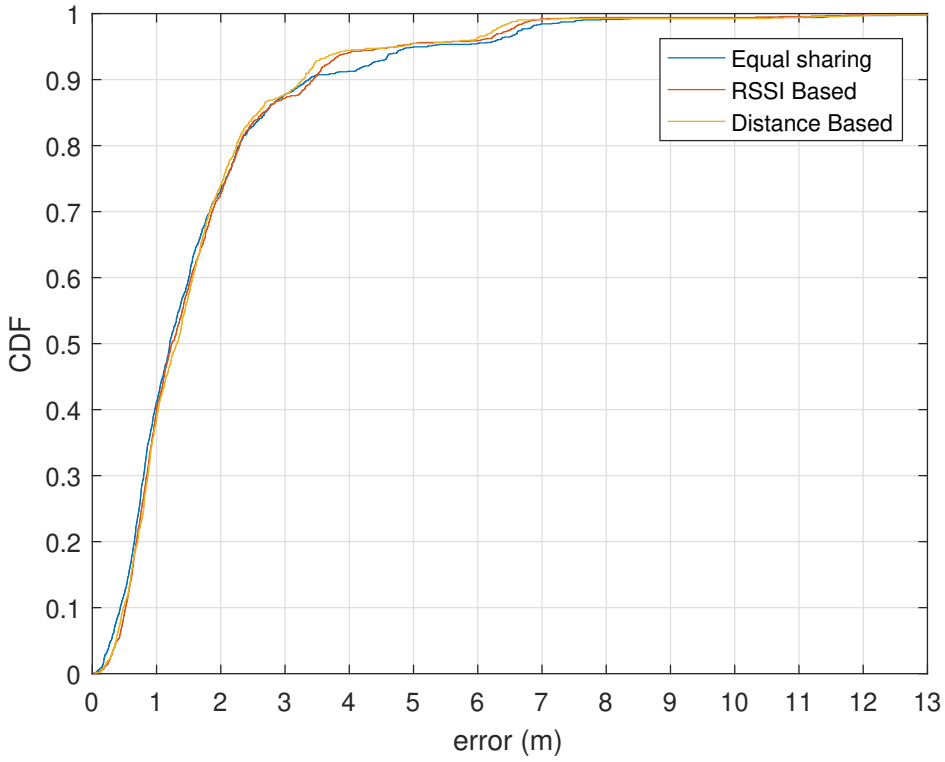


**Figure 5.11** Error CDF of equal sharing and adaptation with $\beta_l = 0.1$, $\beta_m = 0.25$, $\beta_h = 0.4$

The advantage of adaptation based on the distance information with respect to the adaptation based on RSSI can be seen in CDF figures. Improvement with different $\beta_h$, $\beta_m$ and $\beta_l$ levels can also be seen in these figures. When $\beta_h = 0.4$ and $\beta_l$ is kept as in equal sharing, the average error for adaptations based on RSSI quality and distance are below 1m during 40% of the time. The average error is below 2m during 73% of the time for adaptation based on RSSI quality and 75% of the time for adaptation based on the distance. The performance of these values are similar to the performance of equal information sharing. When adaptation is performed with $\beta_h = 0.6$ the estimation performance of both methods seems better. For no-adaptation and RSSI-based adaptation, the estimated probability of the error is below 1m during 40% of the time. On the other hand the performance of adaptation with distance being below 1m is 49% of the time. Furthermore, when $\beta_h$ is increased to 0.8, the estimated probabilities of errors being being below 1m, reach 46% and 50% for RSSI-based and distance-based approaches, respectively.

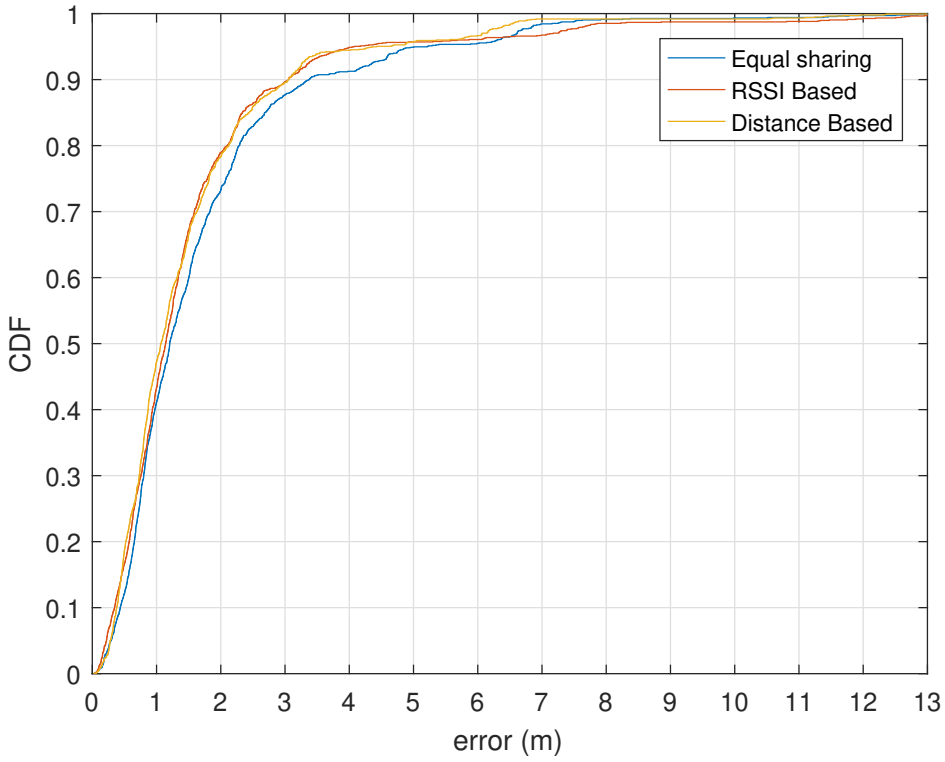


**Figure 5.12** Error CDF of equal sharing and adaptation with $\beta_l = 0.10$, $\beta_m = 0.15$, $\beta_h = 0.6$

As a result, we can say that the adaptation based on RSSI quality and no-adaption provides similar perfomance for the errors below 2m. On the other hand, better CDF performance is seen for the adaptation based on distance. Here there is an exception for the case where $\beta_h = 0.4$. In [18], 1.3 m average error is achieved at 6m $\times$ 6m sized test bed and 1.6 m average error is obtained as the best localization performance among competing teams in the infrastructure-free category in[17].

## 5.5 Simulations with Adaptation of Information Sharing Coefficients with FKF-SCU structure

For this simulations, the algorithm proposed by combination of the FKF-SCU structure for faulty situation and information sharing adaptation both with RSSI quality and distance information is used. Simulations are performed with the data collected at TB2. Again 50% of data is used as training data so as to estimate parameters of (2.13) and localization is performed with remaining 50% of data with faulty scenario

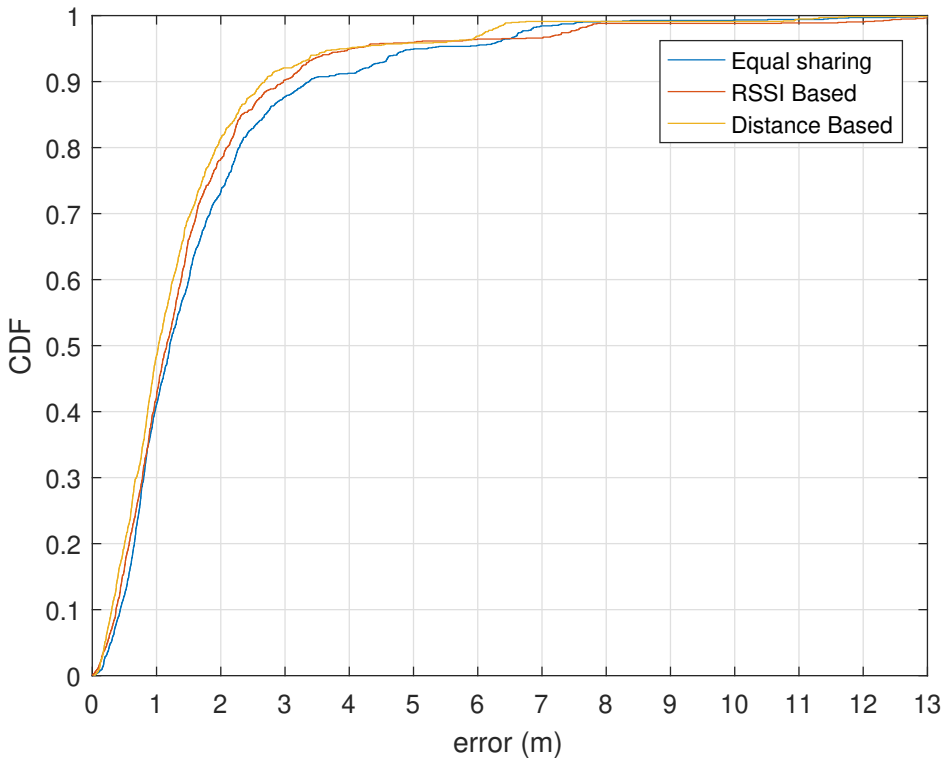


**Figure 5.13** Error CDF of equal sharing and adaptation with $\beta_l = 0.05$, $\beta_m = 0.075$, $\beta_h = 0.8$

described at Section 5.3. During these simulations, FKF is applied with no-reset mode.But whenever a fault is detected faulty estimates are resetted with global estimate to recover the system. In Section 5.3 detection rule is proposed with statistical properties of fingerprint data. Two different threshold levels $1\sigma$ and $3\sigma$ are used with three different information sharing coefficient sets for the simulations for adaptive information sharing and equal (no-adaptation) information sharing. Average mean-square errors gathered from simulation results are shown in Table 5.13-5.18. When these results are compared with the results at Tables 5.10-5.12, there is not a significant performance improvement at average mean-square error. However simulation results show that, adaptive and equal information sharing provides similar performance and there is not a performance degradation even for faulty situation case. Even the results are not at expected level, most important issue is that proposed methods on Section 4.4 and Section 4.5 can be applied together.

**Table 5.13** Average Mean-Square Errors (m) ($\beta_l = 0.1$, $\beta_m = 0.25$, $\beta_h = 0.4$, $1\sigma$)

| Adaptation | $\beta_i = 0.25\ \forall i$ | Adaptive FKF | **Improvement (%)** |
|---|---|---|---|
| RSSI-based | 1.80 | 1.68 | 7.06 |
| Distance-based | 1.80 | 1.77 | 1.78 |

**Table 5.14** Average Mean-Square Errors (m) ($\beta_l = 0.1$, $\beta_m = 0.25$, $\beta_h = 0.4$, $3\sigma$)

| Adaptation | $\beta_i = 0.25\ \forall i$ | Adaptive FKF | **Improvement (%)** |
|---|---|---|---|
| RSSI-based | 1.80 | 1.68 | 6.99 |
| Distance-based | 1.80 | 1.78 | 1.01 |

At first coefficient set, RSSI-based approach provided significantly better result with respect to distance-based adaptation. Furthermore coefficient of healthy measurement combination is increased and improvement also increased as expected. Superiority of RSSI-based adaptation approach continued after second information sharing coefficient set. Among all simulations $1.65m$ average estimation error performance is obtained and the improvement level reached 8.05% level at most in simulations with third coefficient set and $1\sigma$ threshold. As a result we can say that both of the adaptation approaches provided better results with all coefficient sets and threshold levels. The estimated cumulative distribution functions (CDF) of average estima-

**Table 5.15** Average Mean-Square Errors (m) ($\beta_l = 0.1$, $\beta_m = 0.15$, $\beta_h = 0.6$, $1\sigma$)

| Adaptation | $\beta_i = 0.25\ \forall i$ | Adaptive FKF | **Improvement (%)** |
|---|---|---|---|
| RSSI-based | 1.8083 | 1.66 | 7.65 |
| Distance-based | 1.8083 | 1.68 | 7.05 |

**Table 5.16** Average Mean-Square Errors (m) ($\beta_l = 0.1$, $\beta_m = 0.15$, $\beta_h = 0.6$, $3\sigma$)

| Adaptation | $\beta_i = 0.25\ \forall i$ | Adaptive FKF | **Improvement (%)** |
|---|---|---|---|
| RSSI-based | 1.80 | 1.68 | 6.83 |
| Distance-based | 1.80 | 1.69 | 6.39 |

tion errors are shown in Figure 5.14-5.17 for different information-sharing coefficient sets and thresholds. For all cases, the estimated probability of the error is below 1m during around 40% of the time and below $2m$ is between 60%-70% of the time.

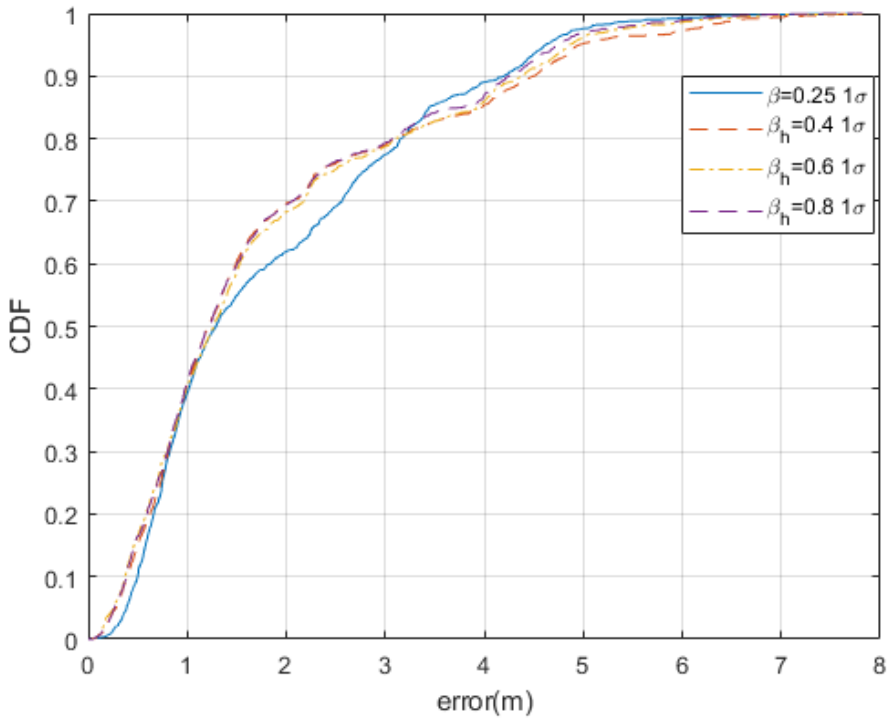


**Figure 5.14** Error CDF of RSSI quality based adaptation with $1\sigma$-FKF-SCU

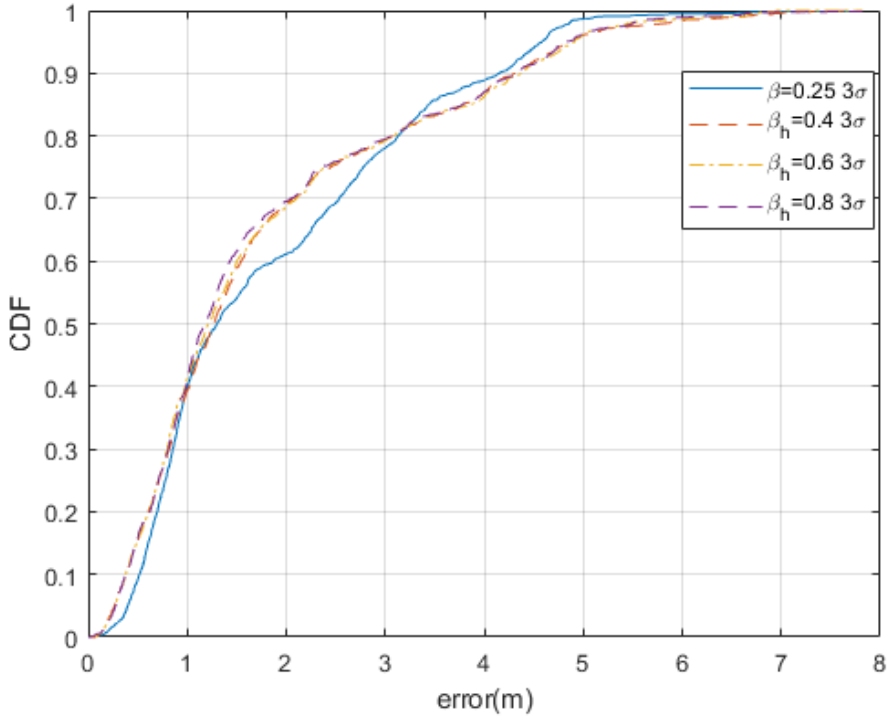


**Figure 5.15** Error CDF of RSSI quality based adaptation with $3\sigma$-FKF-SCU

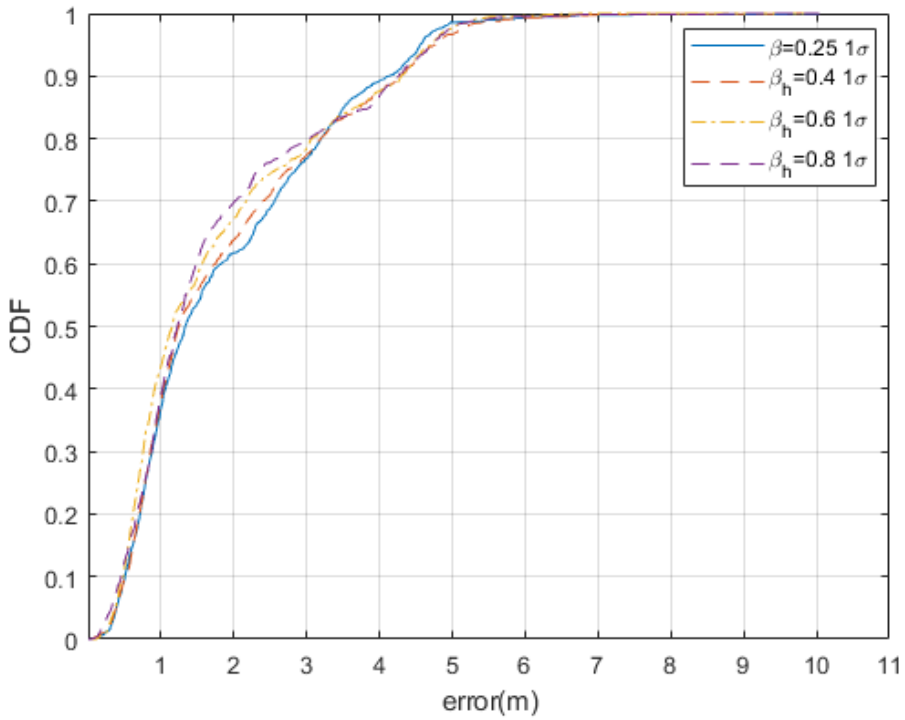


**Figure 5.16** Error CDF of distance based adaptation with $1\sigma$-FKF-SCU

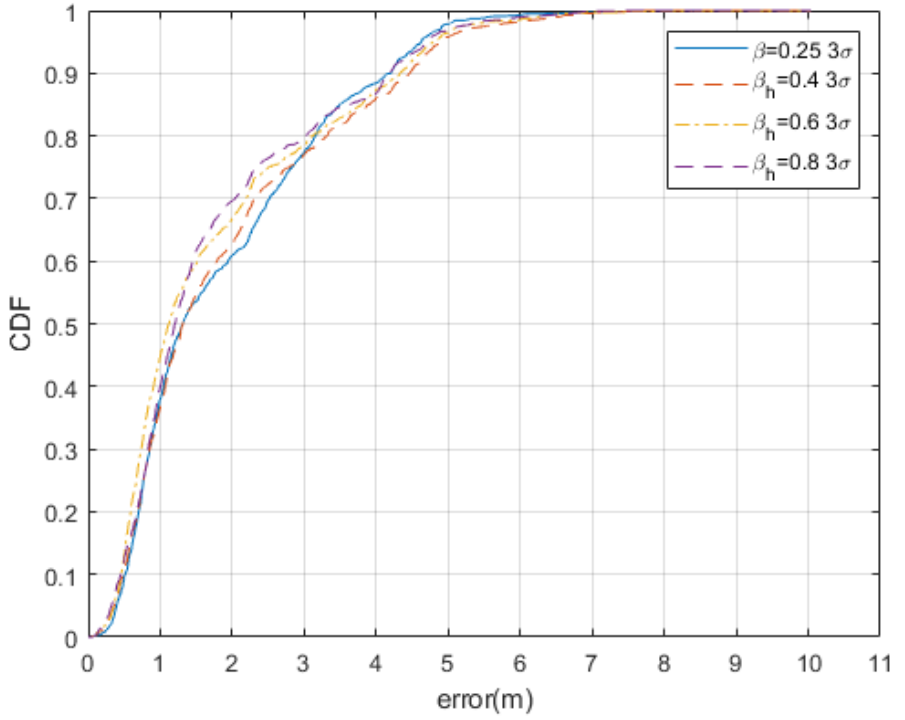


**Figure 5.17** Error CDF of distance based adaptation with $3\sigma$-FKF-SCU

**Table 5.17** Average Mean-Square Errors (m) ($\beta_l = 0.05$, $\beta_m = 0.075$, $\beta_h = 0.8$, $1\sigma$)

| Adaptation | $\beta_i = 0.25\ \forall i$ | Adaptive FKF | **Improvement (%)** |
|---|---|---|---|
| RSSI-based | 1.80 | 1.65 | 8.05 |
| Distance-based | 1.80 | 1.66 | 7.27 |

**Table 5.18** Average Mean-Square Errors (m) ($\beta_l = 0.05$, $\beta_m = 0.075$, $\beta_h = 0.8$, $3\sigma$)

| Adaptation | $\beta_i = 0.25\ \forall i$ | Adaptive FKF | **Improvement (%)** |
|---|---|---|---|
| RSSI-based | 1.80 | 1.66 | 7.43 |
| Distance-based | 1.80 | 1.68 | 6.82 |

The estimated cumulative distribution functions (CDF) of average estimation errors RSSI and distance based adaptation approaches are given together in Figure 5.18-5.20 for different information-sharing coefficient sets and thresholds.

## 5.6 Conclusion

At this chapter set up of two test beds and simulation results of the data fusion methods applied for indoor localization at these test beds are provided. Performance of proposed data fusion methods is compared both with traditional CKF and among each other. During performance evaluation fault tolerance performance is also considered which is not a common issue for other studies in literature. Proposed fault detection rule proved the fault tolerance property of FKF and provided almost same results achieved at no-fault situation at TB1 and TB2. After that two proposed information sharing adaptation methods are assessed with the data collected at TB2. Faulty situation is not considered for this case and better results are gathered with adaptive information sharing coefficients. Lastly FKF-SCU structure is applied with two information sharing adaptation approaches. As a result simulations with all coefficient sets and thresholds provided good results.

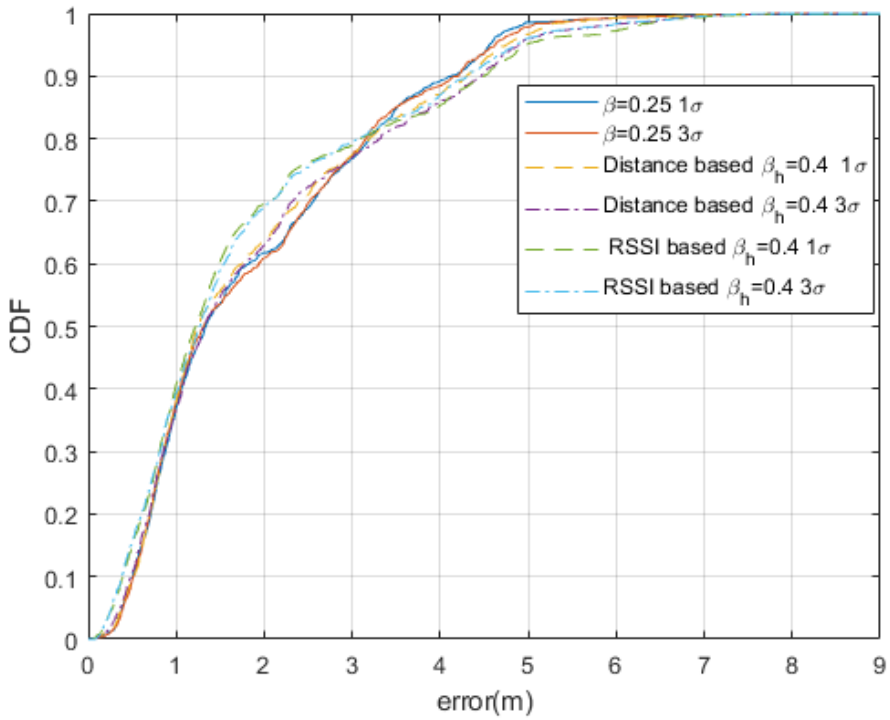


**Figure 5.18** Error CDF of RSSI vs Distance based adaptation for $\beta_h = 0.4$

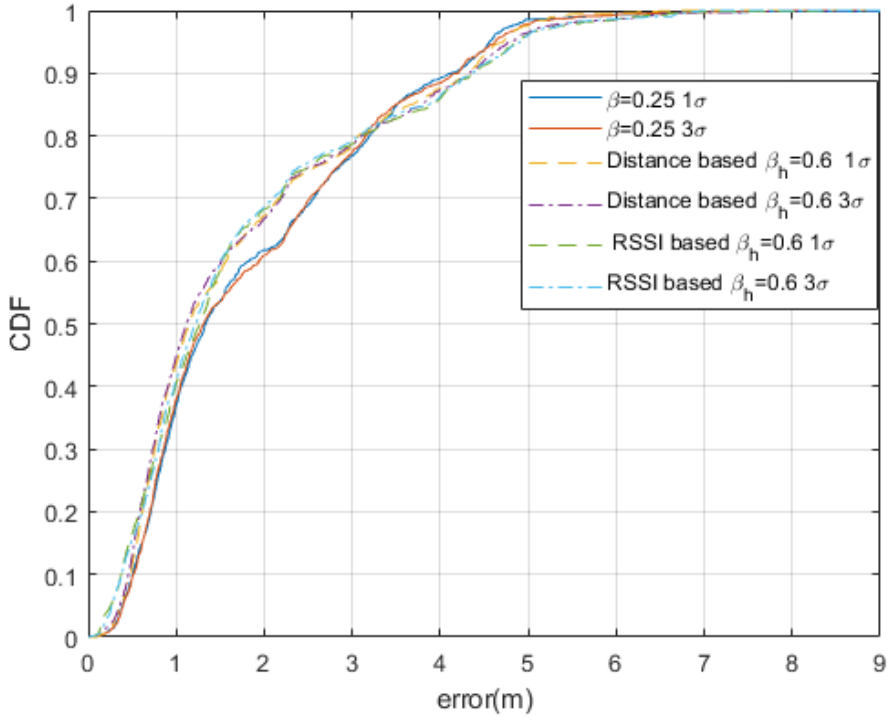


**Figure 5.19** Error CDF of RSSI vs Distance based adaptation for $\beta_h = 0.6$

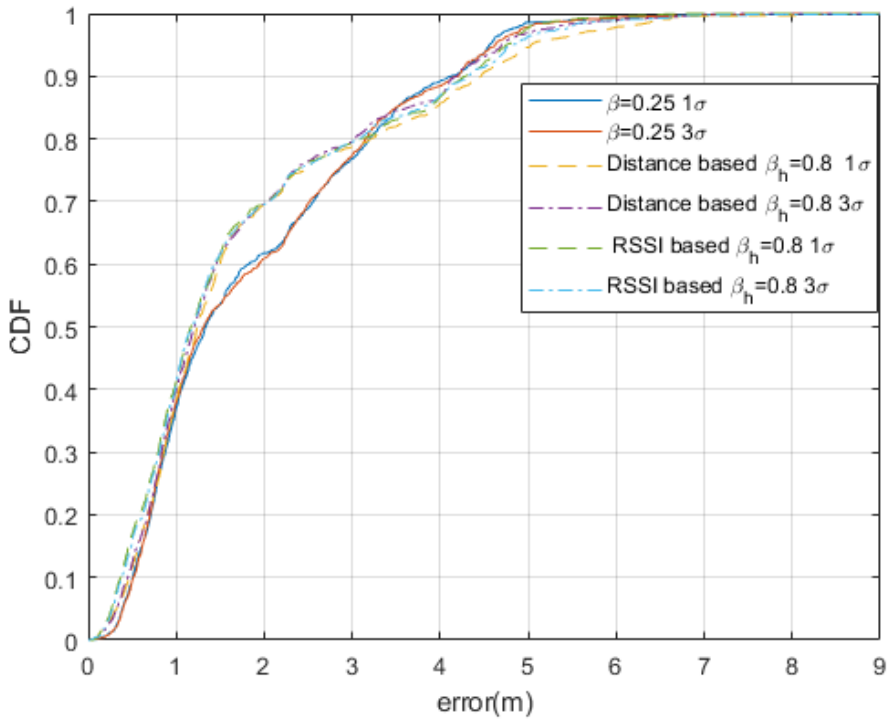


**Figure 5.20** Error CDF of RSSI vs Distance based adaptation for $\beta_h = 0.8$

# 6. CONCLUSION

In this study three different positioning methods for indoor environment are studied. These methods are based on well known position estimation algorithm Kalman filter. Moreover federated Kalman filtering ,one of the alternative Kalman filter configurations, is chosen as sensor fusion structure because of its fault tolerance performance at outdoor positioning applications. At first method a fault tolerant FKF structure is proposed, at which the update of filtered covariance matrix is skipped whenever sensor faults are detected. In the sequel, adaptation of information sharing coefficients is aimed and an adaptive FKF structure is proposed in the no-reset configuration for no-fault situation. Here two adaptation approaches are given for online adjustment of the coefficients. These approaches are based on RSSI readings obtained from APs and the distances gathered via conversion of these RSSI readings. The algorithms are tested on the data obtained from test beds prepared with four access points. The proposed algorithms can drastically improve the localization error performance as compared to a simple lateration using the RSSI data directly or regular CKF and FKF structures. As a result at most 18.29% estimation error improvement is achieved with distance based adaptation approach when $\beta_h = 0.8$. It should be also noted that the proposed approaches can easily be applied in any indoor environment with already deployed access points without additional infrastructure requirements. Lastly another algorithm is proposed by combining fault tolerant configuration and adaptive structure approach. This algorithm is also tested on the real data used for previous methods and at most 8.05% estimation error improvement is achieved with distance based adaptation approach when $\beta_h = 0.8$. On the other hand it is shown that the combination of two different structure worked without performance degradation.

In indoor environment each location has its own path loss characteristics. The measurements collected on the site are used for the calculations of parameter of signal propagation model. We also proposed using of least squares method to estimate the path loss exponent and the multi-path noise parameter for each access point separately. These parameters are calculated with fingerprint (off-line) data and not need to be updated if it is not necessary. Additionally, there is no need to use a localization server to process that data as proposed in [73].

At early stages of the study it is observed that both CKF and FKF cannot tolerate a fault and cannot recover even after the faulty AP starts operating normally. The remedy to this problem is shown to be the federated Kalman filter with skipped covariance updating (FKF-SCU), which provides fault tolerance and rapid system recovery in the presence of a fault via detection of temporary faults (signal interruptions) of the APs. The fault detection method is based on the fingerprint data of the localization environment. Nonetheless, it is also possible to adopt other methods to determine the detection threshold when fingerprint data is not available. On the other hand, prior knowledge about geometry of the localization environment can be also another option to enhance position estimation performance by ignoring the estimates belongs to the outside of the localization area. Assigning the information sharing coefficients to a minimum value , when the estimates from certain local filters become unreliable, is another factor in improving the performance of FKF-SCU. This switching mechanism also en-lighted us to further the studies for other adaptation techniques to take advantage of that property of FKF.

Then another important contribution is provided with the approaches for adaptation of information sharing coefficients. Two different adaptation strategy significantly improved the positioning error performance when compared with equal information sharing strategy. Furthermore, better results are obtained with the approach that makes use of distances gathered via the conversion of RSSI data than adapting the coefficients directly with the raw RSSI data. After getting performance enhancement both with fault tolerance and adaptive configuration, both of these configurations

are combined in a new configuration. As a result an adaptive fault tolerant system is provided for localization applications. The simulation results obtained with this system showed that there is still gap for the improvement of information sharing coefficient adaptation mechanism. At this point machine learning algorithms such as genetic algorithm and fuzzy logic for online adaptation is thought to be useful by monitoring the change in innovation and its covariance of each local filter given at (3.13) and (3.15) respectively. Moreover proposed algorithms can be used for indoor environments deployed with sensors such as BLE, UWB etc. On the other hand, as proof of concept of this study, it is possible to use these methods in a mobile application that can provide online positioning information.

# BIBLIOGRAPHY


[1] R. Zekavat and R. M. Buehrer, *Handbook of Position Location: Theory, Practice and Advances*, 1st ed. Wiley-IEEE Press, 2011.

[2] M. S. Grewal, A. P. Andrews, and C. G. Bartone, *Global navigation satellite systems, inertial navigation, and integration*. John Wiley & Sons, 2013.

[3] D. L. Hall and S. A. McMullen, *Mathematical techniques in multisensor data fusion*. Artech House, 2004.

[4] F. Keresteciogl u, *Change detection and input design in dynamical systems*. Research Studies Press Baldock, Hertfordshire, 1993.

[5] R. J. Patton, "Fault-tolerant control: the 1997 situation," *IFAC Proceedings Volumes*, vol. 30, no. 18, pp. 1029–1051, 1997.

[6] R. Isermann, "Model-based fault-detection and diagnosis–status and applications," *Annual Reviews in control*, vol. 29, no. 1, pp. 71–85, 2005.

[7] D. L. Hall and J. Llinas, "An introduction to multisensor data fusion," *Proceedings of the IEEE*, vol. 85, no. 1, pp. 6–23, 1997.

[8] Y. Gu, A. Lo, and I. Niemegeers, "A survey of indoor positioning systems for wireless personal networks," *IEEE Communications surveys & tutorials*, vol. 11, no. 1, pp. 13–32, 2009.

[9] A. M. Ladd, K. E. Bekris, A. P. Rudys, D. S. Wallach, and L. E. Kavraki, "On the feasibility of using wireless ethernet for indoor localization," *IEEE Transactions on Robotics and Automation*, vol. 20, no. 3, pp. 555–559, 2004.

[10] T. K. Kohoutek, R. Mautz, and A. Donaubauer, "Real-time indoor positioning using range imaging sensors," in *Real-Time Image and Video Processing 2010*, vol. 7724. International Society for Optics and Photonics, 2010, p. 77240K.

[11] L. M. Ni, Y. Liu, Y. C. Lau, and A. P. Patil, "Landmarc: indoor location sensing using active rfid," in *Proceedings of the First IEEE International Conference on Pervasive Computing and Communications, 2003.(PerCom 2003).* IEEE, 2003, pp. 407–415.

[12] M. Kok, J. D. Hol, and T. B. Schön, "Indoor positioning using ultrawideband and inertial measurements," *IEEE Transactions on Vehicular Technology*, vol. 64, no. 4, pp. 1293–1303, 2015.

[13] P. Bahl and V. N. Padmanabhan, "Radar: an in-building rf-based user location and tracking system," in *Proceedings IEEE INFOCOM 2000. Conference on Computer Communications. Nineteenth Annual Joint Conference of the IEEE Computer and Communications Societies (Cat. No.00CH37064)*, vol. 2, 2000, pp. 775–784 vol.2.

[14] H. Liu, H. Darabi, P. Banerjee, and J. Liu, "Survey of wireless indoor positioning techniques and systems," *IEEE Transactions on Systems, Man, and Cybernetics, Part C (Applications and Reviews)*, vol. 37, no. 6, pp. 1067–1080, 2007.

[15] Q. Dong and W. Dargie, "Evaluation of the reliability of rssi for indoor localization," in *2012 International Conference on Wireless Communications in Underground and Confined Areas*. IEEE, 2012, pp. 1–6.

[16] K. Kaemarungsi and P. Krishnamurthy, "Analysis of wlan's received signal strength indication for indoor location fingerprinting," *Pervasive and mobile computing*, vol. 8, no. 2, pp. 292–316, 2012.

[17] D. Lymberopoulos, J. Liu, X. Yang, R. R. Choudhury, V. Handziski, and S. Sen, "A realistic evaluation and comparison of indoor location technologies: Experiences and lessons learned," in *Proceedings of the 14th international conference on information processing in sensor networks*, 2015, pp. 178–189.

[18] T. Dag and T. Arsan, "Received signal strength based least squares lateration algorithm for indoor localization," *Computers & Electrical Engineering*, vol. 66, pp. 114–126, 2018.

[19] J. Röbesaat, P. Zhang, M. Abdelaal, and O. Theel, "An improved ble indoor localization with kalman-based fusion: An experimental study," *Sensors*, vol. 17, no. 5, p. 951, 2017.

[20] L. Yan, B. Liu, and D. Zhou, "Asynchronous multirate multisensor information fusion algorithm," *IEEE Transactions on Aerospace and Electronic Systems*, vol. 43, no. 3, pp. 1135–1146, 2007.

[21] J. Dong, D. Zhuang, Y. Huang, and J. Fu, "Advances in multi-sensor data fusion: Algorithms and applications," *Sensors*, vol. 9, no. 10, pp. 7771–7784, 2009.

[22] C. Harris, A. Bailey, and T. Dodd, "Multi-sensor data fusion in defence and aerospace," *The Aeronautical Journal*, vol. 102, no. 1015, pp. 229–244, 1998.

[23] R. E. Kalman, "A new approach to linear filtering and prediction problems," *Transaction of the ASME—Journal of Basic Engineering*, pp. 35–45, 1960.

[24] I. Skog and P. Handel, "In-car positioning and navigation technologies—a survey," *IEEE Transactions on Intelligent Transportation Systems*, vol. 10, no. 1, pp. 4–21, 2009.

[25] T. Aybakan and F. Kerestecioğlu, "Indoor positioning using federated kalman filter," in *2018 3rd International Conference on Computer Science and Engineering (UBMK)*. IEEE, 2018, pp. 483–488.

[26] T. Ayabakan and F. Kerestecioğlu, "Multi-sensor indoor positioning," in *2019 4th International Conference on Computer Science and Engineering (UBMK)*. IEEE, 2019, pp. 1–6.

[27] D. Willner, C. Chang, and K. Dunn, "Kalman filter algorithms for a multi-sensor system," in *1976 IEEE Conference on Decision and Control including the 15th Symposium on Adaptive Processes*. IEEE, 1976, pp. 570–574.

[28] S.-L. Sun and Z.-L. Deng, "Multi-sensor optimal information fusion kalman filter," *Automatica*, vol. 40, no. 6, pp. 1017–1023, 2004.

[29] H. R. Hashemipour, S. Roy, and A. J. Laub, "Decentralized structures for parallel kalman filtering," *IEEE Transactions on Automatic Control*, vol. 33, no. 1, pp. 88–94, 1988.

[30] M. Wei and K. Schwarz, "Testing a decentralized filter for gps/ins integration," in *IEEE Symposium on Position Location and Navigation. A Decade of Excellence in the Navigation Sciences*. IEEE, 1990, pp. 429–435.

[31] Y. Gao, E. Krakiwsky, M. Abousalem, and J. McLellan, "Comparison and analysis of centralized, decentralized, and federated filters," *Navigation*, vol. 40, no. 1, pp. 69–86, 1993.

[32] N. A. Carlson, "Federated filter for fault-tolerant integrated navigation systems," in *IEEE PLANS'88., Position Location and Navigation Symposium, Record.'Navigation into the 21st Century'*. IEEE, 1988, pp. 110–119.

[33] ——, "Federated square root filter for decentralized parallel processors," *IEEE Transactions on Aerospace and Electronic Systems*, vol. 26, no. 3, pp. 517–525, 1990.

[34] Z. Chen, H. Zou, H. Jiang, Q. Zhu, Y. Soh, and L. Xie, "Fusion of wifi, smartphone sensors and landmarks using the kalman filter for indoor localization," *Sensors*, vol. 15, no. 1, pp. 715–732, 2015.

[35] Z.-A. Deng, Y. Hu, J. Yu, and Z. Na, "Extended kalman filter for real time indoor localization by fusing wifi and smartphone inertial sensors," *Micromachines*, vol. 6, no. 4, pp. 523–543, 2015.

[36] G. Chen, X. Meng, Y. Wang, Y. Zhang, P. Tian, and H. Yang, "Integrated wifi/pdr/smartphone using an unscented kalman filter algorithm for 3d indoor localization," *Sensors*, vol. 15, no. 9, pp. 24 595–24 614, 2015.

[37] A. Abdulqader Hussein, T. A. Rahman, and C. Y. Leow, "Performance evaluation of localization accuracy for a log-normal shadow fading wireless sensor network under physical barrier attacks," *Sensors*, vol. 15, no. 12, pp. 30 545–30 570, 2015.

[38] L.-h. Lv and H.-x. Jin, "A fusion location algorithm based on federated kalman filtering," in *2016 4th International Conference on Machinery, Materials and Computing Technology*. Atlantis Press, 2016, pp. 2001–2005.

[39] X. Xu, F. Pang, Y. Ran, Y. Bai, L. Zhang, Z. Tan, C. Wei, and M. Luo, "An indoor mobile robot positioning algorithm based on adaptive federated kalman filter," *IEEE Sensors Journal*, vol. 21, no. 20, pp. 23 098–23 107, 2021.

[40] R. Harle, "A survey of indoor inertial positioning systems for pedestrians," *IEEE Communications Surveys & Tutorials*, vol. 15, no. 3, pp. 1281–1293, 2013.

[41] F. Seco, A. R. Jiménez, C. Prieto, J. Roa, and K. Koutsou, "A survey of mathematical methods for indoor localization," in *2009 IEEE International Symposium on Intelligent Signal Processing*. IEEE, 2009, pp. 9–14.

[42] R. Mautz and S. Tilch, "Survey of optical indoor positioning systems," in *2011 international conference on indoor positioning and indoor navigation*. IEEE, 2011, pp. 1–7.

[43] D. Dardari, P. Closas, and P. M. Djurić, "Indoor tracking: Theory, methods, and technologies," *IEEE Transactions on Vehicular Technology*, vol. 64, no. 4, pp. 1263–1278, 2015.

[44] H.-S. Kim, D.-R. Kim, S.-H. Yang, Y.-H. Son, and S.-K. Han, "An indoor visible light communication positioning system using a rf carrier allocation technique," *Journal of lightwave technology*, vol. 31, no. 1, pp. 134–144, 2012.

[45] S. De Lausnay, L. De Strycker, J.-P. Goemaere, B. Nauwelaers, and N. Stevens, "A survey on multiple access visible light positioning," in *2016 IEEE International Conference on Emerging Technologies and Innovative Business Practices for the Transformation of Societies (EmergiTech)*. IEEE, 2016, pp. 38–42.

[46] A. Bekkali, H. Sanson, and M. Matsumoto, "Rfid indoor positioning based on probabilistic rfid map and kalman filtering," in *Third IEEE International Conference on Wireless and Mobile Computing, Networking and Communications (WiMob 2007)*. IEEE, 2007, pp. 21–21.

[47] C. Laoudias, M. P. Michaelides, and C. G. Panayiotou, "Fault tolerant positioning using wlan signal strength fingerprints," in *2010 International Conference on Indoor Positioning and Indoor Navigation*. IEEE, 2010, pp. 1–8.

[48] C. Laoudias, M. P. Michaelides, and C. Panayiotou, "Fault tolerant fingerprint-based positioning," in *2011 IEEE International Conference on Communications (ICC)*. IEEE, 2011, pp. 1–5.

[49] A. Chennaka, "Fault tolerant indoor localization using wi-fi," Ph.D. dissertation, Iowa State University, 2015.

[50] N. B. Priyantha, "The cricket indoor location system," Ph.D. dissertation, Massachusetts Institute of Technology, 2005.

[51] A. Harter and A. Hopper, "A distributed location system for the active office," *IEEE network*, vol. 8, no. 1, pp. 62–70, 1994.

[52] A. Ward, A. Jones, and A. Hopper, "A new location technique for the active office," *IEEE Personal communications*, vol. 4, no. 5, pp. 42–47, 1997.

[53] Y.-S. Kuo, P. Pannuto, K.-J. Hsiao, and P. Dutta, "Luxapose: Indoor positioning with mobile phones and visible light," in *Proceedings of the 20th annual international conference on Mobile computing and networking*. ACM, 2014, pp. 447–458.

[54] F. Zafari, A. Gkelias, and K. K. Leung, "A survey of indoor localization systems and technologies," *IEEE Communications Surveys & Tutorials*, 2019.

[55] M. Bolic, M. Rostamian, and P. M. Djuric, "Proximity detection with rfid: A step toward the internet of things," *IEEE Pervasive Computing*, vol. 14, no. 2, pp. 70–76, 2015.

[56] C. Peng, G. Shen, Y. Zhang, Y. Li, and K. Tan, "Beepbeep: a high accuracy acoustic ranging system using cots mobile devices," in *Proceedings of the 5th*

*international conference on Embedded networked sensor systems*. ACM, 2007, pp. 1–14.

[57] J. Hightower and G. Borriello, "A survey and taxonomy of location sensing systems for ubiquitous computing," *UW CSE*, pp. 01–08, 2001.

[58] D. Zhang, F. Xia, Z. Yang, L. Yao, and W. Zhao, "Localization technologies for indoor human tracking," in *2010 5th International Conference on Future Information Technology*. IEEE, 2010, pp. 1–6.

[59] Z. Yang, Z. Zhou, and Y. Liu, "From rssi to csi: Indoor localization via channel response," *ACM Computing Surveys (CSUR)*, vol. 46, no. 2, p. 25, 2013.

[60] G. Zanca, F. Zorzi, A. Zanella, and M. Zorzi, "Experimental comparison of rssi-based localization algorithms for indoor wireless sensor networks," in *Proceedings of the workshop on Real-world wireless sensor networks*. ACM, 2008, pp. 1–5.

[61] M. Sugano, T. Kawazoe, Y. Ohta, and M. Murata, "Indoor localization system using rssi measurement of wireless sensor network based on zigbee standard." *Wireless and Optical Communications*, vol. 538, pp. 1–6, 2006.

[62] Z. Jianyong, L. Haiyong, C. Zili, and L. Zhaohui, "Rssi based bluetooth low energy indoor positioning," in *2014 International Conference on Indoor Positioning and Indoor Navigation (IPIN)*. IEEE, 2014, pp. 526–533.

[63] A. S. Paul and E. A. Wan, "Rssi-based indoor localization and tracking using sigma-point kalman smoothers," *IEEE Journal of Selected Topics in Signal Processing*, vol. 3, no. 5, pp. 860–873, 2009.

[64] M. Youssef and A. Agrawala, "The horus wlan location determination system," in *Proceedings of the 3rd international conference on Mobile systems, applications, and services*. ACM, 2005, pp. 205–218.

[65] A. Neskovic, N. Neskovic, and G. Paunovic, "Modern approaches in modeling of mobile radio systems propagation environment," *IEEE Communications Surveys & Tutorials*, vol. 3, no. 3, pp. 2–12, 2000.

[66] R. Akl, D. Tummala, and X. Li, "Indoor propagation modeling at 2.4 ghz for ieee 802.11 networks." in *wireless and optical communications*. International Association of Science and Technology for Development, 2006, pp. 1–6.

[67] T. S. Rappaport *et al.*, *Wireless communications: principles and practice*. prentice hall PTR New Jersey, 1996, vol. 2.

[68] V. Cantón Paterna, A. Calveras Auge, J. Paradells Aspas, and M. A. Perez Bullones, "A bluetooth low energy indoor positioning system with channel diversity, weighted trilateration and kalman filtering," *Sensors*, vol. 17, no. 12, p. 2927, 2017.

[69] N. A. Carlson and M. P. Berarducci, "Federated kalman filter simulation results," *Navigation*, vol. 41, no. 3, pp. 297–322, 1994.

[70] Y. Bar-Shalom, X. R. Li, and T. Kirubarajan, *Estimation with applications to tracking and navigation: theory algorithms and software*. John Wiley & Sons, 2004.

[71] T. Ayabakan, *Indoor Environment WIFI-RSSI Data Set*. Mendeley Data, 2021.

[72] T. AYABAKAN and F. KERESTECIOGLU, "Wi-fi rssi data set for indoor localization," 2021. [Online]. Available: https://dx.doi.org/10.21227/dpne-5785

[73] K. Chintalapudi, A. Padmanabha Iyer, and V. N. Padmanabhan, "Indoor localization without the pain," in *Proceedings of the sixteenth annual international conference on Mobile computing and networking*. Association for Computing Machinery, Inc., 2010, pp. 173–184.

## CURRICULUM VITAE

**Personal Information**

Name Surname : Tarık AYABAKAN

**Education**

Undergraduate Education : Turkish Naval Academy,2008
Graduate Education, MSc : Yıldız Technical University,2014
Foreign Language Skills : English (92.5/100 YDS 2021)

**Work Experience**

Name of Employer and Dates of Employment: Turkish Naval Forces, 30th Aug 2008-

**Publications derived from the thesis**

Journal papers:

- T. Ayabakan and F. Kerestecioğlu, "RSSI-Based Indoor Positioning via Adaptive Federated Kalman Filter," in IEEE Sensors Journal, doi:10.1109/JSEN.2021.3097249.

Conference papers:

- T. Ayabakan and F. Kerestecioğlu, "Indoor positioning using federated Kalman Filter," 2018 26th Signal Processing and Communications Applications Conference (SIU), 2018, pp. 1-4, doi: 10.1109/SIU.2018.8404427.

- T. Aybakan and F. Kerestecioğlu, "Indoor Positioning Using Federated Kalman Filter," 2018 3rd International Conference on Computer Science and Engineering (UBMK), 2018, pp. 483-488, doi: 10.1109/UBMK.2018.8566652.

- T. Ayabakan and F. Kerestecioğlu, "Multi-Sensor Indoor Positioning," 2019 4th International Conference on Computer Science and Engineering (UBMK), 2019, pp. 1-6, doi: 10.1109/UBMK.2019.8907082.